Journal of Sea Research 192 (2023) 102362

Contents lists available at ScienceDirect

Journal of Sea Research

journal homepage: www.elsevier.com/locate/seares

Gross pelagic primary production in the Ems-Dollard estuary

A.G. Brinkman (Bert)[a,*], P. Jacobs (Pascalle)[a,b]

[a] Wageningen Marine Research, PO Box 57, 1780 AB Den Helder, The Netherlands
[b] Aquaculture in Delta Areas, HZ University of Applied Sciences, Edisonweg 4, 4382 NW Vlissingen, the Netherlands

ARTICLE INFO

Keywords:
Suspended matter
Long-term changes
North Sea
Turbidity
Eutrophication

ABSTRACT

Anthropogenic changes to estuaries, usually highly productive systems, may result in increased turbidity levels, suppress pelagic primary production and negatively affect ecosystem functions.

The Ems-Dollard estuary, enclosed between the Netherlands and Germany, is such an estuary with a long history of human induced changes. From the mid-19th century until 1992, discharges of potato starch and strawboard industry waste water, with high contents of organic matter, negatively affected oxygen concentrations and increased nutrient levels of the system. The growing awareness of the deteriorating effects of these discharges on the ecosystem invoked a large research program, BOEDE, between 1976 and 1980.

The aim of the current paper was to establish the recent gross pelagic primary production, to compare the results with the late seventies data and to relate possible changes to environmental variables such as suspended matter and nutrients.

To this end, six stations from the North Sea into the inner area of the Dollard were visited 39 times in 2012–2013. During each sampling cruise, a so-called PocketBox, containing a number of sensors, provided a high spatial data resolution between stations. At each station, samples were collected for carbon fixation incubations using ^{14}C.

Average chlorophyll-a concentrations as reported in this study were lower compared to 1978–1980 for the seaward stations, and higher for the most inward station in 2012 and almost similar in 2013. Light attenuation coefficients in the outer areas were lower in 2012–2013 (1.22 m^{-1}) compared to the values reported in the period 1976–1980 (1.59 m^{-1}), indicating somewhat less turbid conditions. For the two other stations, light attenuation coefficients in the present study were similar to the late seventies' values, for the station near the entrance of the Ems River in the Ems-Dollard area, the coefficient was substantially higher.

Pelagic primary production in the 2012–2013 period was about 120 g C m^{-2} y^{-1}, mainly determined by the most seaward areas. The largest differences in gross primary production in the current study compared to the 1976–1980 period were found at the seaward stations where production in the late seventies was about 60% higher. In the Dollard-area, production hardly changed since the late seventies, but also stations near the Ems-river entrance into the Ems-Dollard area showed a clear decrease. Changes at the inward stations are to be contributed to an increased turbidity; the decrease at the outer areas to a decreased nutrient level, especially dissolved phosphorus and silicate, but possibly also nitrogen.

1. Introduction

Estuaries were strikingly defined by Pritchard (1967) as "semi-enclosed coastal bodies of water with a free connection to the open sea and within which seawater is measurably diluted with fresh water derived from land drainage". These systems are generally considered to be highly productive systems. This high productivity is attributed to their high nutrient concentrations and many sources of organic carbon including pelagic and benthic autochthonous production and riverine inputs (Cloern, 1987), providing food for higher trophic levels.

In these systems, the contribution of pelagic primary production to the total organic carbon pool can however seriously be depressed by turbidity. Although high turbidity is an intrinsic characteristic of estuarine systems, caused by SPM loads from rivers, resuspension of bottom material (Cloern, 1987) and marine inputs (Postma, 1961; Wang et al., 2012), human activities like dredging and coastal development result in

* Corresponding author.
E-mail addresses: bert.brinkman@brinkman-bab.nl (A.G. Brinkman), pascalle.jacobs@hz.nl (P. Jacobs).

https://doi.org/10.1016/j.seares.2023.102362
Received 2 December 2022; Received in revised form 5 February 2023; Accepted 5 February 2023
Available online 9 February 2023

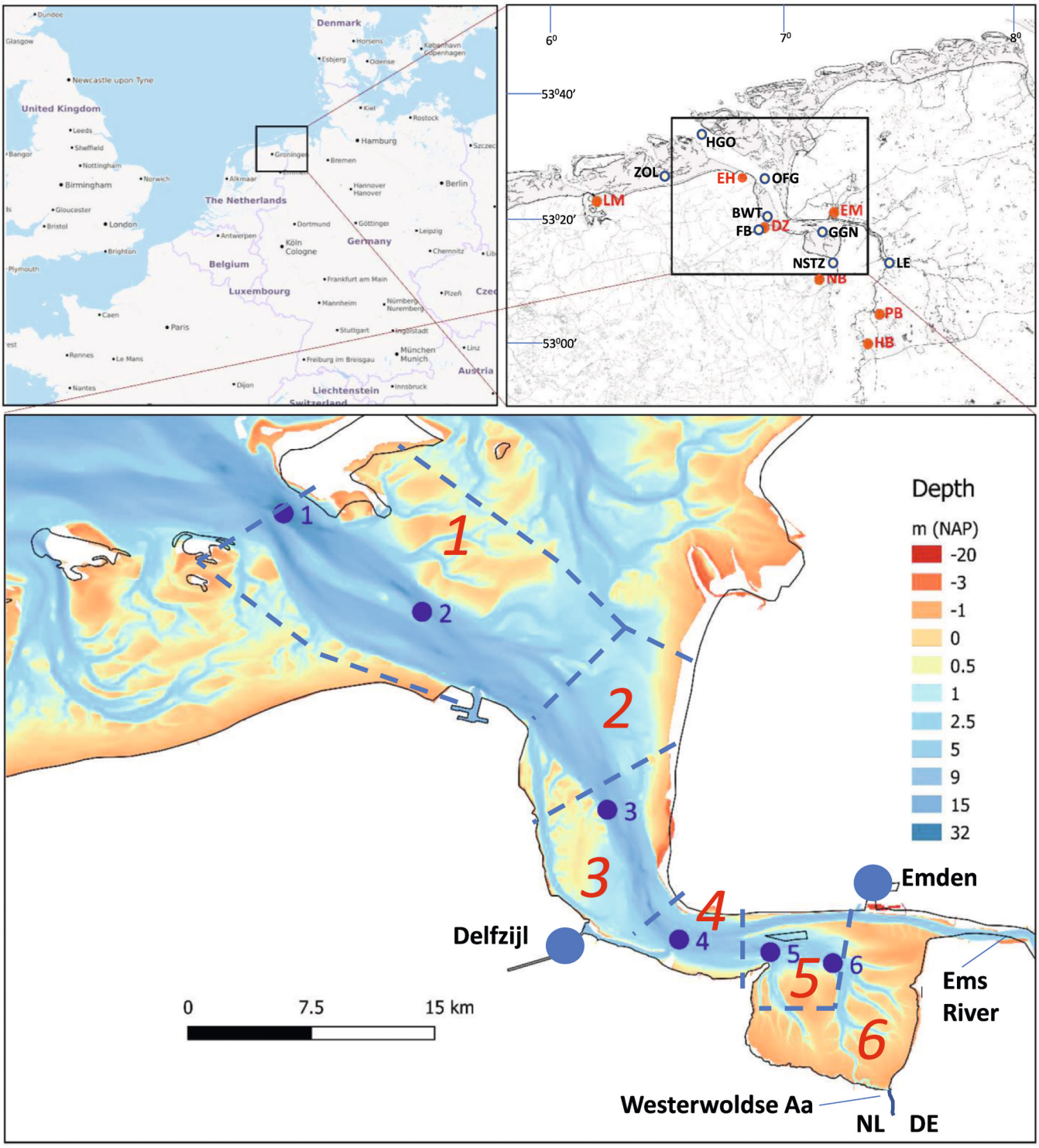

Fig. 1. Ems-Dollard research area, its position in NW-Europe, and more in detail on a depth map (in m NAP, Dutch Ordinary Level). Distinguished compartments (1–6) dashed, numbered in red. Pelagic monitoring sites in this study are marked in blue. Latitude (North) and longitude (East) mentioned in upper right figure. (For interpretation of the references to colour in this figure legend, the reader is referred to the web version of this article.)
Upper right figure: LM = Lauwersmeer, NB = Nieuw Beerta (both weather station sites). Monitoring sites (in black): ZOL = Zuid-oost Lauwers, HGO=Huibert Gat oost, OFG = Oostfriese gaatje, BWT = Bocht van Watum, FB = Farnssum Brug, at the Eems-canal, GGN = Grote Gat Noord, NST = Nieuw Statenzijl. Other relevant sites (in red): EH = Ems Harbour (Eemshaven), EM = Emden, DZ = Delfzijl, PB = Papenburg (all four important harbour sites; the last three also largest cities in the area), HB=Herbrum: site in the Ems-river with a weir, here the river estuary starts. Map source: Open Street Map (OSM, 2021), depth source: Rijkswaterstaat (NL) and Bundes Anstalt für Wasser und Hydrographie (DE). Lower map: monitoring sites in this study (in blue): 1 = Huibert Gat Oost, 2 = Westereems, 3 = OostFriese gaatje, 4 = Bocht van Watum Zuid, 5 = Monding Dollard, 6 = Grote Gat Noord.

Table 1
Some characteristics of the Ems-Dollard area. Compnr denotes the compartment from Fig. 1, "Colijn area" are the combined compartments as used by Colijn (1983). Areas in km^2 and average sediment level in m relative to NAP (Amsterdam Ordnance Datum). See text for precise definition of tidal flats (TF) and channels (CH).

Compnr	Colijn area	Average sediment level TF	Average sediment level CH	Area TF	Area CH	Tot Area	% TF
1	Outer	−0.24	−8.95	73.15	131.99	205.1	35.7
2	Outer	−0.45	−5.11	18.26	49.35	67.6	27.0
3	Mid	−0.54	−7.05	29.30	32.44	61.7	47.5
4	Mid	−0.63	−6.70	4.95	14.43	19.4	25.5
5	Inner	−0.17	−4.52	17.11	11.25	28.4	60.3
6	Inner	0.30	−3.15	58.39	5.66	64.0	91.2
Sum/Average		−0.29	−5.91	201.15	245.12	446.3	45.1

Table 2
Some characteristics of the Ems-Dollard area (continued). High water (HW)- and low water (LW)-volume give the volumes at average high and low water of tidal flats (TF) and channels (CH), respectively. Ditto for depth. See text for precise definition of tidal flats and channels. Average tidal level in m relative to NAP (Amsterdam Ordnance Datum). Tidal level and range in m; volumes in million m^3.

Compnr	Colijn area	Average Tidal Level	Tidal Range	LW_Vol TF	LW_Vol CH	HW_Vol TF	HW_Vol CH	Mean_Vol_TF	Mean_Vol_CH	Mean_Vol_Syst
1	Outer	0.19	2.60	0	1.02E+03	1.12E+02	1.37E+03	5.60E+01	1.20E+03	1.25E+03
2	Outer	0.13	2.91	0	1.83E+02	3.49E+01	3.27E+02	1.75E+01	2.55E+02	2.72E+02
3	Mid	0.15	3.31	0	1.77E+02	6.44E+01	2.84E+02	3.22E+01	2.31E+02	2.63E+02
4	Mid	0.15	3.31	0	7.37E+01	1.13E+01	1.22E+02	5.65E+00	9.79E+01	1.04E+02
5	Inner	0.01	3.25	0	3.26E+01	3.06E+01	6.92E+01	1.53E+01	5.09E+01	6.62E+01
6	Inner	0.01	3.25	0	8.67E+00	7.73E+01	2.70E+01	3.87E+01	1.78E+01	5.65E+01
Sum/ Average		0.11	3.1	0	1.50E+03	3.31E+02	2.19E+03	1.66E+02	1.85E+03	2.01E+03

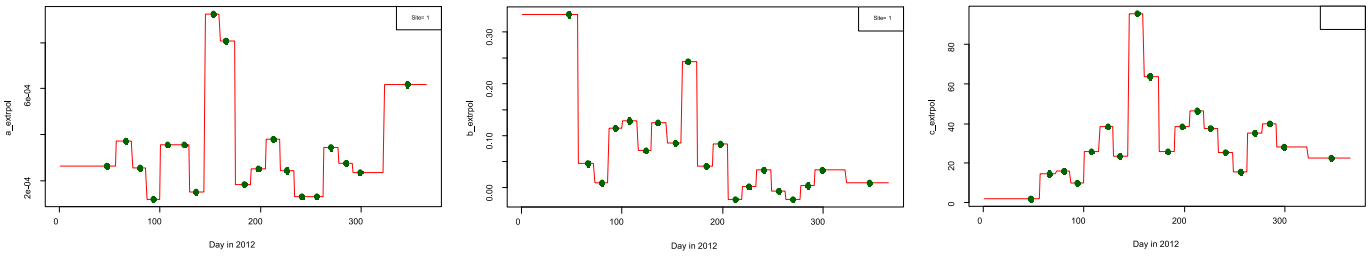

Fig. 2. Extrapolation of available Eilers-Peeters-parameters (a, b and c) to whole-year values, assuming that each value represents the period around the sampling date. Results for station 1 in 2012. First and last values are assumed to be valid from the beginning and to the end of the period, respectively.

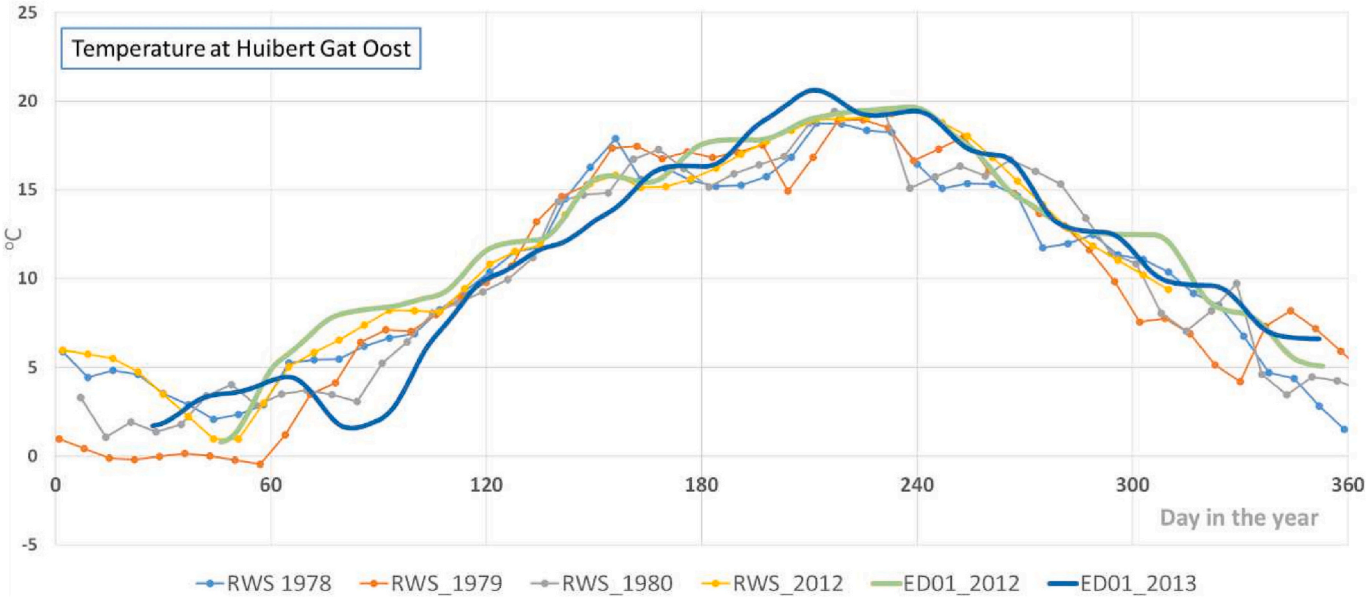

Fig. 3. Temperature at Huibert Gat Oost (site 1, Fig. 1) in 1978–1980 and 2012 according to RWS-monitoring data (RWS, 2017), and interpolated data from this research (ED01_2012 and ED01_2013).

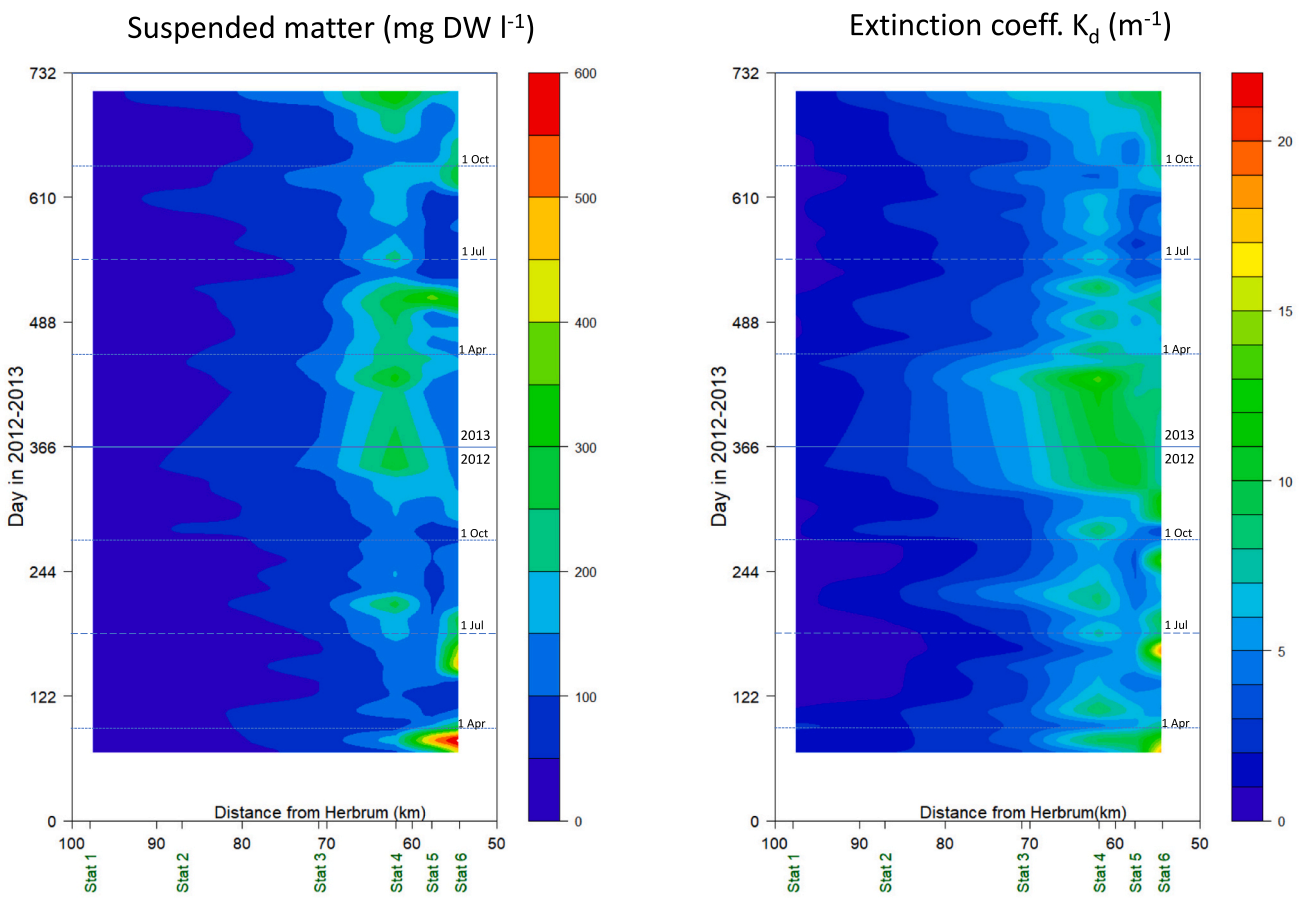

Fig. 4. Left: suspended matter (mg DW l^{-1}) and right: light attenuation coefficient K_d (m^{-1}) in the estuary in 2012–2013 (lower to top). Stations are mentioned, as is the distance from the Ems-river weir at Herbrum.

Table 3
Several average state variables for all stations, years 2012–2013. Temperature in °C, the light attenuation coefficient K_d in m^{-1}, nutrients N, P and Si in µmol l^{-1} and O_2 in mg l^{-1}. O_2-sat in % of oxygen saturation value. Chlorophyll-a (chla) in µg l^{-1}. Salinity in mg l^{-1}. Suspended matter (Susp Matt, as dry matter) in mg l^{-1}.

Station	1	2	3	4	5	6
Temp	10.70	10.61	10.67	10.81	11.06	11.28
K_d	1.22	2.07	4.17	7.59	6.42	8.03
Susp Matt	25.02	43.73	83.68	199.49	138.02	179.24
NH_4-N	5.8	7.8	7.1	5.6	5.8	7.1
NO_2-N	7.1	1.1	1.6	1.4	1.4	1.4
NO_3-N	17	30	83	110	116	117
NO_3NO_2-N	18	31	84	112	117	121
PO_4-P	0.77	1.23	2.41	2.81	7.79	2.97
Si	12	21	63	86	97	103
chla	5.18	6.85	5.89	6.81	5.08	6.45
Salinity	29.56	28.15	22.24	18.58	17.34	16.28
O_2	9.20	9.16	9.14	9.03	9.11	8.99
O_2 -sat	98.37	95.94	92.63	89.70	90.40	90.10

increased turbidity (De Jonge et al., 2014).

Other threats to estuaries that alter the contribution of the different carbon sources and thus the carrying capacity of these systems include eutrophication, pollution and changed freshwater discharge (Kennish, 2002) as well as processes linked to climate change including increased temperatures and sea-level rise (Kennish, 2002).

The Ems-Dollard estuary, enclosed between the Netherlands and Germany (Fig. 1), is the last true estuary of the Dutch part of the Wadden Sea, since all other fresh water inflow to the Wadden Sea is controlled by sluices and pumping stations. The estuary is recognised as an import nature area, with salt marshes at the edges and it is an important area for birds (Heath and Evans, 2000) and seals (Galatius et al., 2022). The area also has a long history of human induced changes, starting as early as the 16th with agricultural land reclamations which lasted until the 19th century (Essink and Esselink, 1998).

An important characteristic in the relatively recent past concerns the discharges of potato starch and straw-board industry waste water, with high contents of organic matter and nutrients (Eggink, 1965, Essink, 1978; Van Arkel, 1977; Essink and Esselink, 1998; Essink, 2003 *in* Compton et al., 2017). This industry started in the mid-19th century, causing large problems in canals and the marine environment. In the mid-1950s, it was realised that measures were needed, and from the beginning of the 1970s waste water, after some pre-purification, was discharged to the estuary, just north of Delfzijl (Fig. 1). Closing factories, changing process methods, and installing waste water treatment plans, caused an ongoing decrease in the organic load to the estuary. From 1992, organic waste discharge had almost come to a halt (Essink and Esselink, 1998).

A second phenomenon concerns the historical changes in nutrient levels in the estuary but also in the rest of the Netherlands. From roughly the beginning of the 1950s, discharges of phosphates and nitrogen compounds increased drastically, followed by legal actions in the 1970s resulting in a decrease from the beginning of the '80s. Phosphorus discharges decreased a lot more that those of nitrate and ammonium. Van Raaphorst and De Jonge (2004) described the changes in these decades for the Lake IJssel (IJsselmeer) and the resulting changes in the discharges into the western Dutch Wadden Sea.

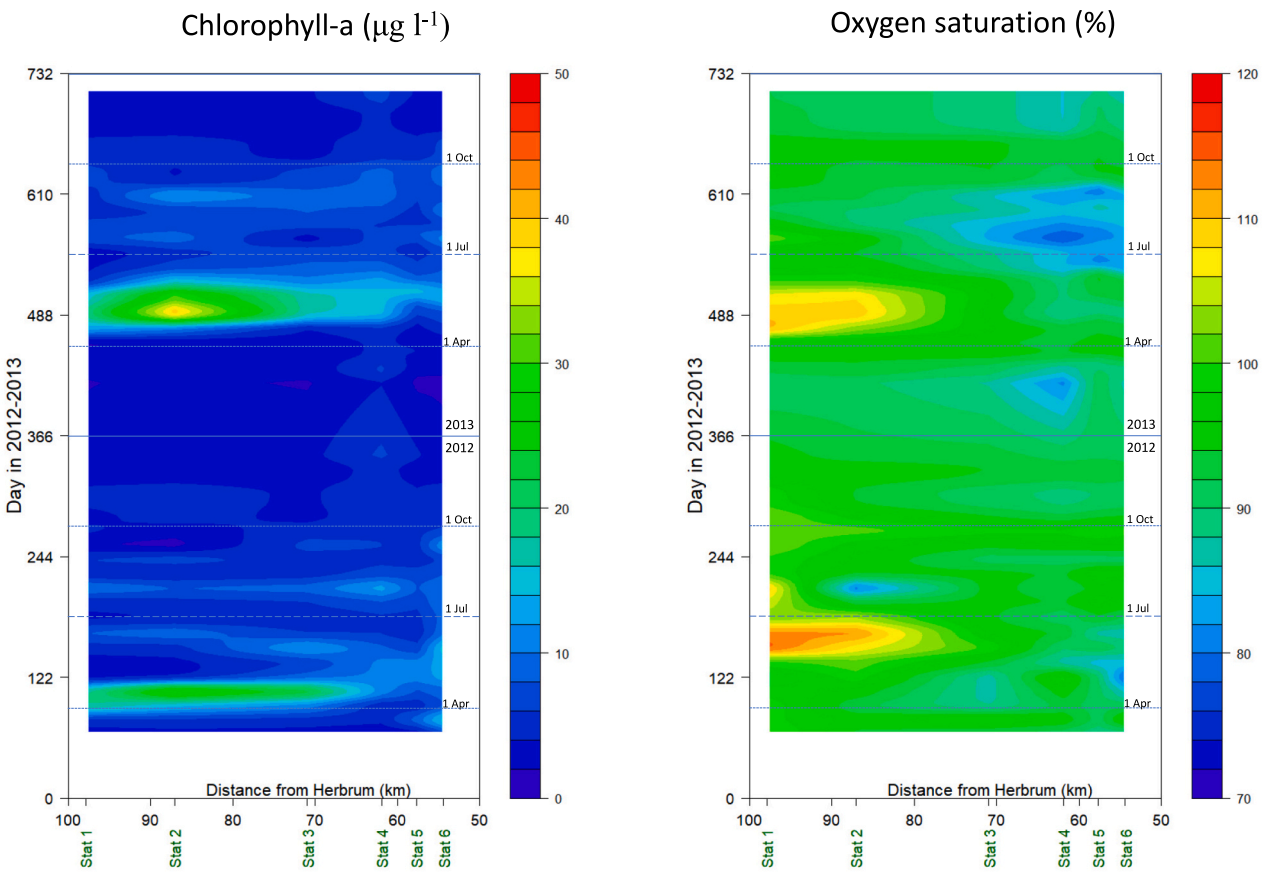

Fig. 5. Left: Chla concentration (µg chla l^{-1}) and right: oxygen saturation (%) in the estuary in 2012–2013 (lower to top) at 1 m depth. Stations are mentioned, as is the distance from the Ems-river weir at Herbrum.

A third phenomenon regards the building of ports and dredging of channels to allow large ships to reach the ports of Eemshaven and Emden and the shipyard in Papenburg. These activities, that started roughly 60 years ago, have affected the hydrodynamical characteristics of the system (Talke and De Swart, 2006). "The Inner Ems has become an efficient sediment trap where high concentrations of fine suspended sediment are known to accumulate (Talke and De Swart, 2006). Furthermore, the estuarine turbidity zone in the Ems-Dollard has become hyper turbid since the 1990s" (Van Maren et al., 2015).

These historic and ongoing alterations have also altered the ecological characteristics of the system (Talke and De Swart, 2006). There is a recent recognition of the uniqueness of the area and an ambitious nature restoration program is initiated (ED2050, 2021).

There are, however, great concerns that the high turbidity levels will continue to negatively affect the pelagic primary production and thus the amount of food available for higher trophic levels. And, that this high turbidity will hamper the return of characteristic elements including shellfish reefs. The fear is that the current vulnerable state of this system has greatly reduced the resilience to cope with additional present and future stressors resulting from climate change (RWS, 2017). The inducement for the study presented here was to establish the current pelagic primary production in the area.

1.1. Aim

Between 1976 and 1980, the area was the centre of a large research program (BOEDE) investigating the effect of the wastewater effluent on benthic and pelagic gross primary production (Colijn, 1983; Baretta and Ruardij, 1988). Since then, research in the area has been scarce (De Jonge and Schückel, 2019; Jacobs et al., 2021). Aim of this paper was to establish the recent gross pelagic primary production, to compare the results to primary production in the late seventies and relate the changes to changes in environmental variables including suspended matter, chlorophyll-a and nutrients.

2. Study area

The Ems-Dollard estuary (Fig. 1) comprises almost 450 km^2 including tidal flats and channels. The area is characterised by a sharp gradient in salinity, nutrients and turbidity, with at the North Sea side relatively clear water due to a low suspended matter content (about 20 mg l^{-1}), a relatively high salinity (about 28‰) and low nutrient concentrations, while at the inland part (the Dollard) water is very turbid with suspended matter concentrations up to a few hundred mg l^{-1}, a low salinity (5‰) due to the freshwater input from the rivers Ems and, to a lesser extent, the Westerwoldse Aa and relatively high nutrient concentrations (Colijn, 1983; De Jonge and Brauer, 2006; Brinkman et al., 2014).

The average high-water depth decreases from slightly over 5 m in the outer areas to about 1 m in the Dollard area regarding the whole compartment. Channel depths at low water decrease from >15 m in the outer areas to <1 m in the Dollard area. In the Dollard, almost the complete area runs dry at low water, with an average emersion period of 43%. Close to the North Sea, the sediment has a low silt content (grain size <63 µm); this is up to 100% in the Dollard (RIKZ, 1998; EasyGSh-DB Projekt, 2020). In Table 1 and Table 2 some system characteristics are summarized.

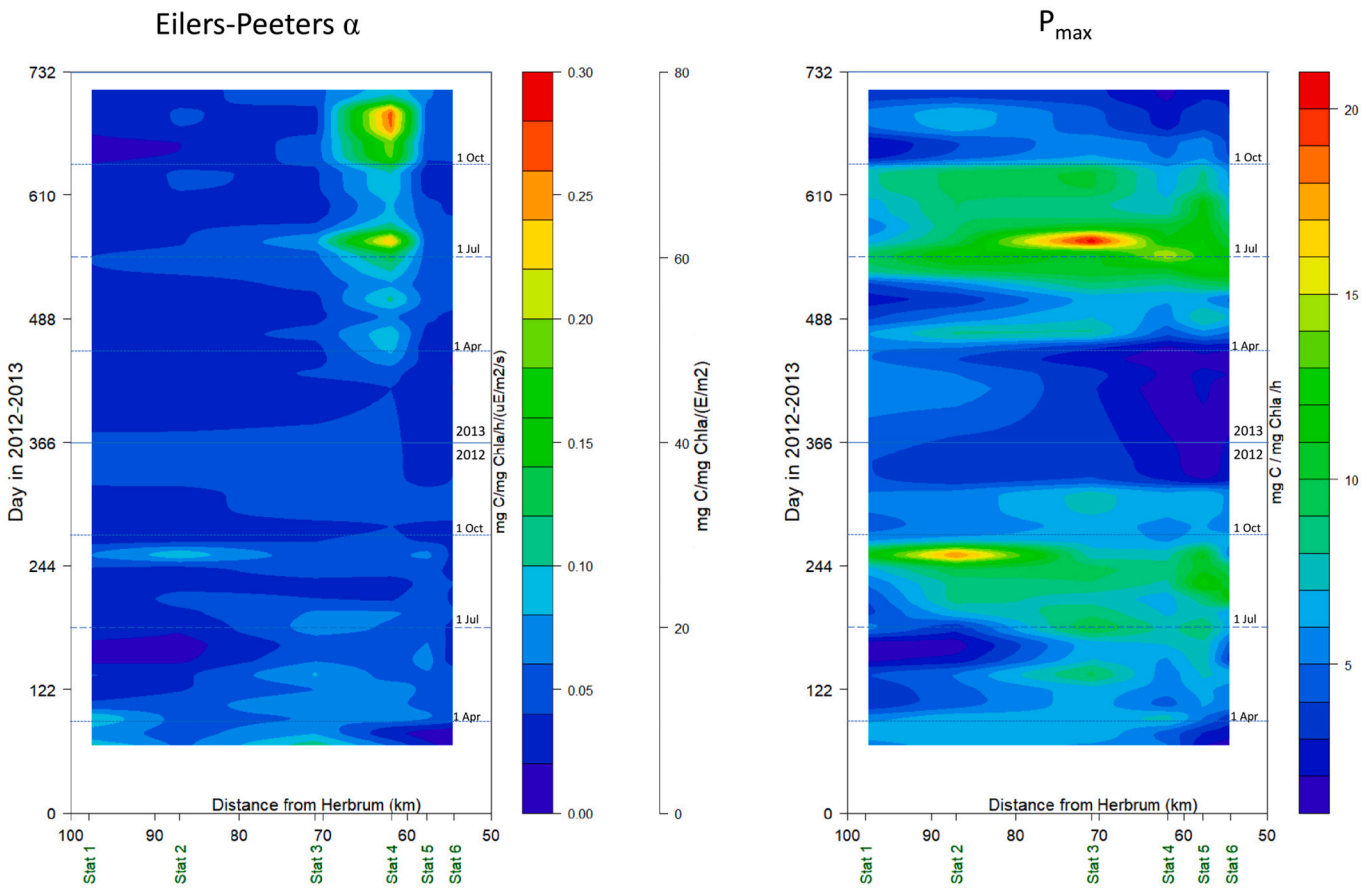

Fig. 6. Left: steepness of P—I curve at low light intensities (Eilers-Peeters α^B, mg C (mg chla)$^{-1}$ h^{-1} (μE m^{-2})$^{-1}$ and mg C (mg chla)$^{-1}$ (μE m^{-2})$^{-1}$ (second scale bar)). Right: maximum productivity per unit of chlorophyll (P^B_{max}, mg C (mg chla)$^{-1}$ h^{-1})).
Results for both years 2012–2013 (lower to top).

3. Methods

3.1. Field sampling

Six stations from the North Sea into the inner area of the Dollard (Fig. 1) were visited 20 times in 2012 and 19 times in 2013 by boat. Exact sampling dates are listed in Table A1 (appendix A). Surface water samples were taken at 1 m depth using a pressure pump. On board, subsamples were taken and stored, and conductivity, temperature and oxygen content were measured directly; these three variables were also measured directly in the water column.

Stored samples were brought to the laboratory in a cooled and dark container and analysed the same day for carbon uptake using ^{14}C incubation experiments (see next section). From the results, daily and yearly gross pelagic production values for the whole estuary were computed. The remaining water subsamples were filtered on board for chlorophyll-a, suspended matter and nutrient analysis. For chlorophyll-a (chla), between 50- and 400-ml water sample was filtered over a GF/F filter, filters were then wrapped in labelled aluminum foil and kept between −20 and − 80 °C until further processing. Samples were taken in duplicate. For suspended matter analysis, between 50 and 400 ml water sample was filtered over pre-weighted GF/C filters and stored at 4 °C until further processing. Samples were taken in duplicate. For nutrients, 250 ml water sample was filtered over 0.45 μm Polydisk filters and stored at 4 °C until further processing (See the appendix C for more analysis details).

All sampling started at station 1, usually about two hours after high tide, and ended about 4.5 h later at station 6. Since high tide times at station 6 are about 2.5 h after those at station 1, final sampling times generally were about one hour before low tide.

The underwater vertical light climate (from surface to the sediment surface) was assessed at each station using a Licor underwater quantum sensor with a second sensor measuring the atmospheric radiation level (Licor, 2022) (For details see appendix C). Solar radiation was available on an hourly basis for two stations (Lauwersmeer and Nieuw-Beerta, Fig. 1) (KNMI, 2021).

During all cruises, a so-called PocketBox (4h-Jena Engineering, 2021) was installed on board. While sailing from sampling site 1 up to site 6 (Fig. 1) apart from the hand-measurements mentioned above at each station, temperature, conductivity, turbidity, light attenuation, and content of oxygen, chlorophyll-a, yellow substance and coloured dissolved matter were recorded continuously, thereby providing a high spatial resolution of these data (details in appendix C).

Apart from vertical light profile assessments, sampling of deeper waters was not done.

3.2. Primary productivity

Carbon uptake rates were measured at the Royal Netherlands Institute for Sea Research (NIOZ), Texel, by filling 8 flasks with 50 ml of water sample and spiked with 80 μl ^{14}C-bicarbonate with an activity of approximately 0.5 Mbq ml^{-1}. Three additional flasks were filled with 200 ml filtered seawater and 80 μl labelled ^{14}C, these flasks remained under the fume hood during the incubation of the flasks filled with water sample, and were used to establish the actual activity added. The 8 sample flasks were incubated under light intensities varying from 0 to 900 μE m^{-2} s^{-1} (cf. Colijn, 1983; Riegman et al., 1990; Riegman and Colijn, 1991). Light intensity inside each flask was measured using a

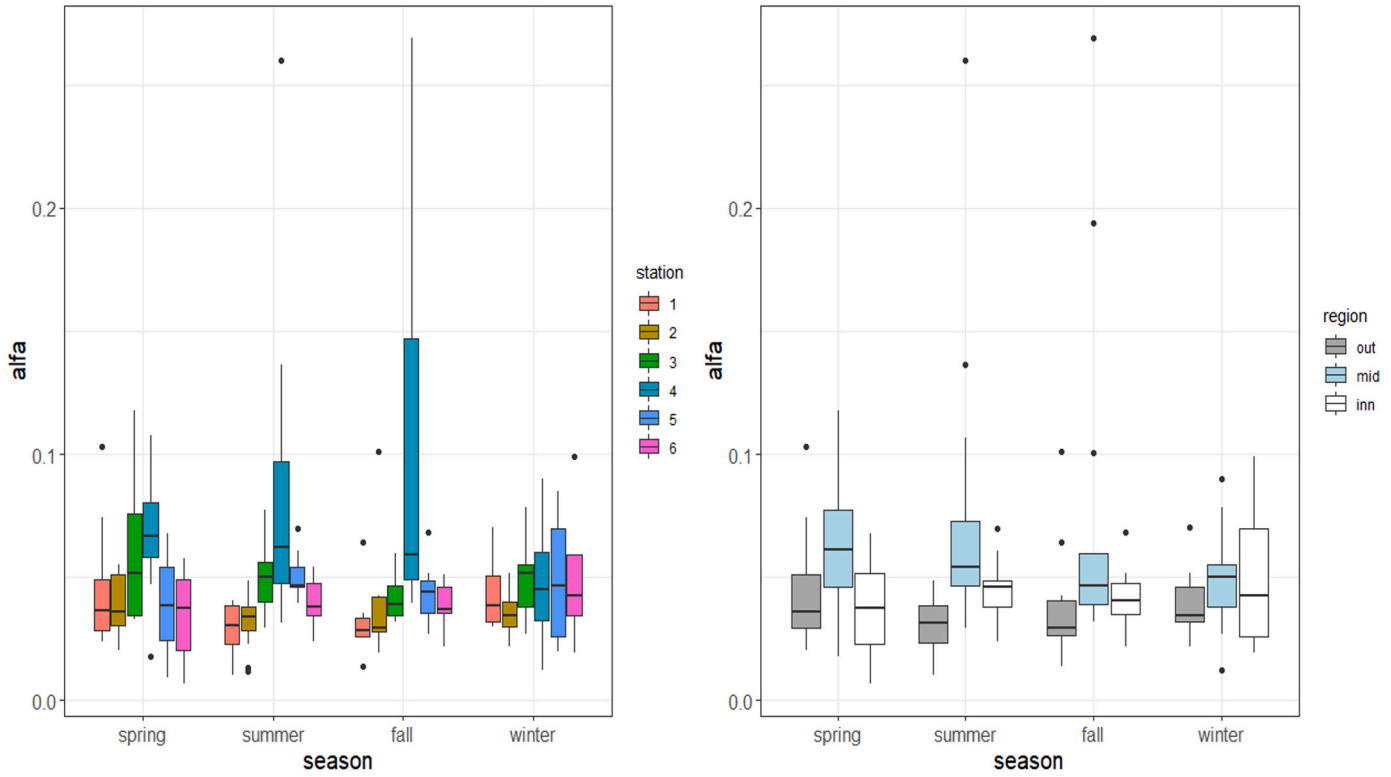

Fig. 7. Left: steepness of P—I curve at low light intensities (Eilers-Peeters α^B, mg C (mg chla)$^{-1}$ h^{-1} (μE m^{-2})$^{-1}$ as derived from the 2012 and 2013 measurements), for each station showing the differences between seasons. Outlier of 0.8 removed from analysis (station 1, 16 Feb 2012).
Right: α^B pooled for all 6 stations showing the differences between seasons.

spheric light sensor (Walz Spherical Micro Quantum Sensor US-SQS/L; Waltz, 2022). The incubation temperature was set to in-situ water temperatures and controlled by a water bath. Samples were incubated for two hours, after which the uptake of carbon was stopped by adding HCl to each flask. Samples were filtered over a GF/F filter and left in an exicator for at least one hour. To each flask, including the controls, 10 ml of scintillation fluid was added and left overnight. The next day, activity was measured as DPM (disintegration rate per minute).

Dissolved inorganic carbon (DIC, mg l^{-1}) was measured, as alkalinity, on GF/F filtered water using a titration (cf. Strickland and Parsons, 1972).

The carbon fixation rate (CP; mg C l^{-1} h^{-1}) per sample was calculated according to eq. (1):

$$CP = \left(\frac{(DPM_{sample} - DPM_{dark})\ DIC \bullet 1.05 \bullet T_{corr}}{DPM_{added} \bullet t} \right) \quad (\text{mg C l}^{-1}\ \text{h}^{-1}) \qquad (1)$$

where '*added*' indicates the ^{14}C amount added derived from the average of the 3 control vials, '*sample*' the amount after 2 h and 'DMP *dark*' the amount in the dark bottle after 2 h. The value of 1.05 is a correction factor for the preference of the microbiologically relevant enzyme Rubisco for the ^{12}C atom over the ^{14}C atom. Since field values for the temperature T occasionally differed between sampling sites while incubation temperatures were the same for all samples, T_{corr} accounts for differences between field and incubation temperature.

The chlorophyll-specific fixation rates PP(I) (or: primary productivity as a function of light intensity (I) (mg C (mg chla)$^{-1}$ h^{-1}) then follows from PP(I) = CP / (mg chla l^{-1}), using the chla-content analysed for each sample (see appendix C for details on the analysis method).

3.3. Production light curves

Production-light PP(I) curves for each sample were fitted using the model by Eilers and Peeters (Eilers and Peeters, 1988):

$$PP(I) = \frac{I}{aI^2 + bI + c} \quad (\text{mg C (mg chla)}^{-1}\ \text{h}^{-1}) \qquad (2)$$

Parameters a, b and c were computed using a non-linear least square method (NLS) (Bates and Chambers, 1992) from the R-library (R Core Team, 2021). The a-value allows for an optimum in the PI-curve, and the 1/c equals the initial slope of the PI-curve (See appendix C for a further explanation). Parameters a and b have no specific biological meaning. Together with c they determine the maximum productivity.

$$P_{max} = \frac{1}{2\sqrt{ac} + b} \quad (\text{mg C (mg chla)}^{-1}\ \text{h}^{-1}) \qquad (2a)$$

3.4. Under water light climate

Calculating the integrated production in the water column requires the light climate in the water column, chlorophyll-a content from the water sample analyses and hourly irradiation values. The latter were taken from the Royal Netherlands Meteorological Institute (KNMI, 2021) for stations Lauwersoog and Nieuw-Beerta (LM and NB, respectively, in Fig. 1), weighted per station depending on the distance of a station to these weather stations. For light conversion factors see appendices A and C.

Vertical light profiles (I_z versus depth z) were analysed following Lambert-Beer's equation:

$$I_z = I_0 exp(-K_d\ z) \quad (\text{W m}^{-2}) \qquad (3)$$

where I_0 is the light intensity right below the water surface and K_d the light attenuation coefficient (m^{-1}). I_0 does not equal solar irradiation because of reflection at the surface and uncertainties due to waves, and had to be estimated (See appendix C for details).

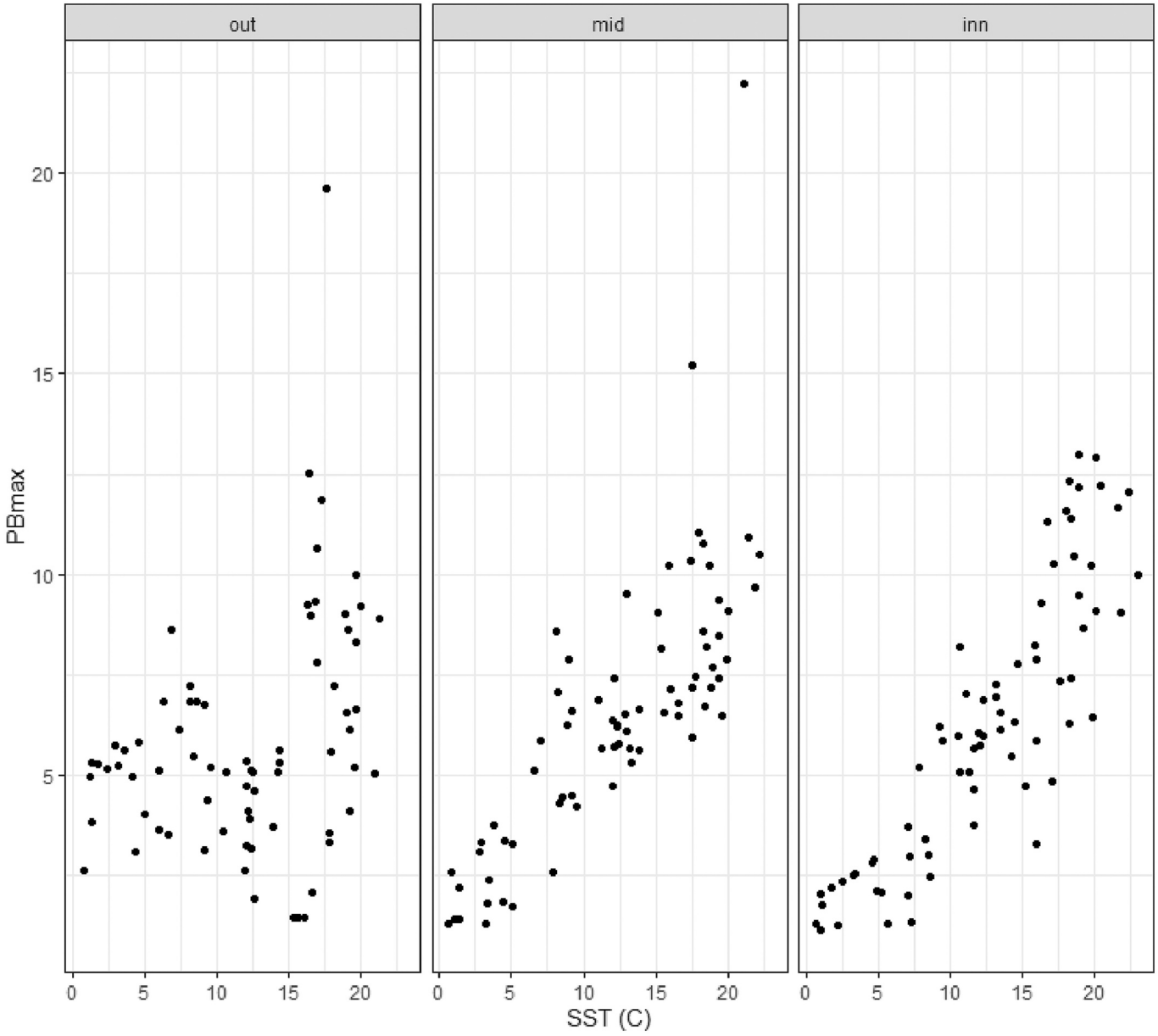

Fig. 8. P^{B}_{max} values (mg C (mg chla) $^{-1}$ h^{-1}) for station groups (outer = 1 + 2; mid = 3 + 4; inner = 5 + 6), as a function of observed temperature (°C).

3.5. Daily rates per station

From the analyses above, the production per unit of chlorophyll-a and its light dependency PP(I) is known. Light intensity in the water column at each depth z (I_z) is computed according to eq. (3) and from this, the productivity PP(I_z) at each depth. Chla-concentrations and temperature are assumed to be constant over depth.

For each sampling moment, the production in the water column at each depth z is.

$$Prod\ (z) = PP(I_z) \bullet chla \bullet F(Temp) \quad \left(\text{mg C m}^{-3}\ \text{h}^{-1}\right) \tag{4}$$

The temperature dependency function F(Temp) is described in appendix C. To compute the production per m^2, Prod(z) is integrated over depth; this is done numerically:

$$ProdSite = \sum_{z=0}^{z=H} Prod(z) \quad \left(\text{mg C m}^{-2}\ \text{h}^{-1}\right) \tag{5}$$

where H is the local depth (m).

3.6. Extrapolation/interpolation estuary per year

The derived field data and incubation results, plus solar radiation data from KNMI (KNMI, 2021), allow an estimation of the system production for 2012 and 2013, according to Eqs. (4) and (5).

For this, it was assumed that primary productivity parameters for each sampling site were representative for the whole associated compartment of the estuary (Fig. 1).

Depth data were available (Fig. 1) from Rijkswaterstaat (NL) and the Bundes Anstalt für Wasser und Hydrographie (DE), and tidal data (on a 10-min basis, RWS, 2017) were analysed. Area with >5% emersion period were considered as tidal area; the other part is considered as channel (Table 1). It implies that in reality, channel areas partly may run dry, and tidal areas not always run dry completely. For channels and tidal areas in each subarea, primary production was computed for each hour of the day using to eq. (5), accounting for water levels varying between low- and highwater. For tidal areas, the fraction of the time the area is submerged is taken into account. As a result, the average production in tidal areas is much lower than the one at high tide, roughly ¼

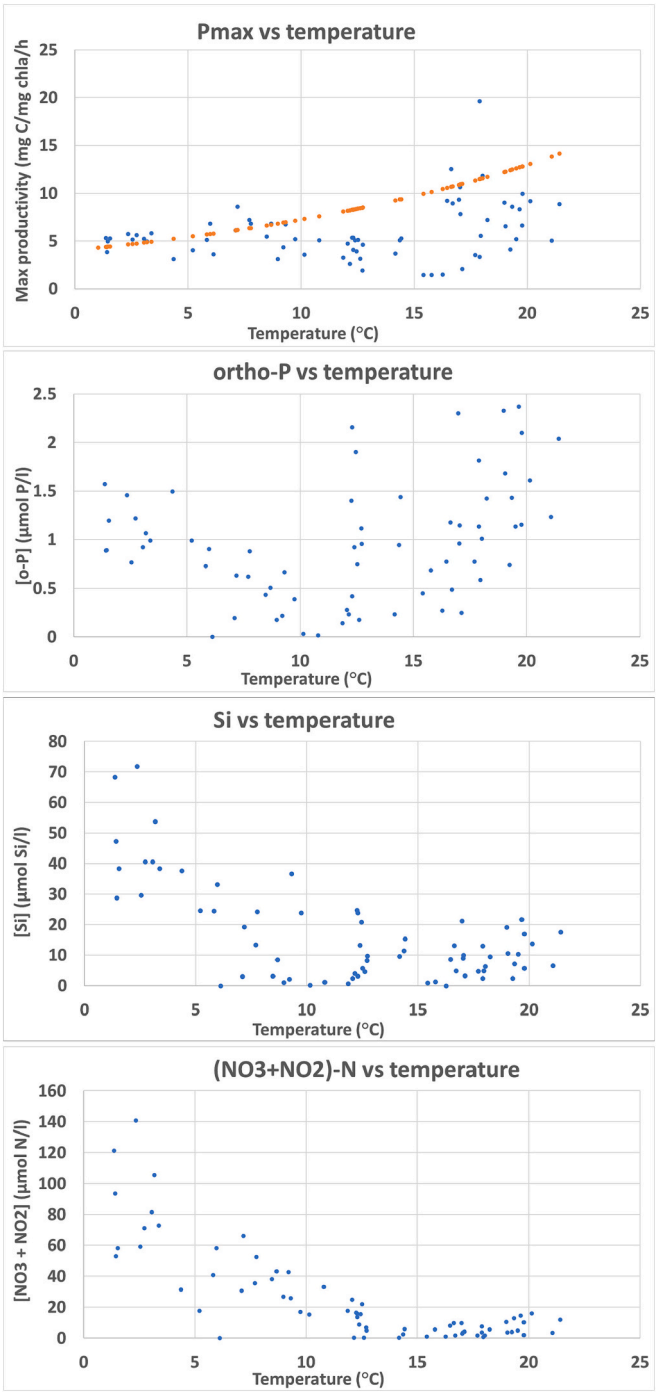

Fig. 9. Maximum productivity P^B_{max} (mg C (mg chla) $^{-1}$ h^{-1}) vs temperature for the outer two stations (1 + 2), in the months January–August of 2012 and 2013 (upper graph), including the line roughly connecting the maximum values for P^B_{max} vs T. Other graphs show ortho-phosphate, silicate and (nitrate + nitrite) content in the same period. For the dashed line in the upper graph, we used $P^B_{max} = 13*1.06^{(Temp-20)}$ The values of 13 and 1.06 were estimated by eye, finding a line that roughly marked the maximum of P^B_{max}.

of that maximum value. Including tidal and subtidal area sizes, gross primary production values ProdComp(d,c) for day d and compartment c were estimated.

Computing ProdSite and ProdComp on all other days needs an inter- and extrapolation of the Eiler-Peeters parameter values (a, b and c) for the whole period [2012−2013]. Since a, b and c are correlated, separate interpolation is not correct. Therefore, the set (a, b, c) is assumed to be valid for the periods around the sampling day. The first values are also used for the whole initial period of the 2012, and the last values for the last period of 2013. Fig. 2 gives an example for 2012 alone.

Extinction coefficient K_d -values were interpolated for days between two successive observations in time using moving averages.

With all inter- and extrapolated parameters and hourly solar radiation data, daily primary production ProdComp was computed for each compartment and each day in 2012 and 2013. Together with the subarea sizes (Table 1), these total daily production values per compartment yield daily system primary production data (g C d^{-1}); summed for all days and all compartments it yields system gross primary production figures (ProdCompYear) for both years (kg C y^{-1}).

4. Results

4.1. State variables

Temperature patterns were as customary for this area, with highest values in July–August. Values for the seaward station 1 are shown in Fig. 3, including data for 1978–1980 and 2012 by RWS (RWS, 2017), illustrated that most years roughly are averages, and thus, the 2012–2013 years were not substantially different from the years 1977–1980. A few exceptions were 1979 (cold winter period) and 2013 (cold second half of March) (see also appendix D, Fig. D1).

Suspended (organic plus *inorganic) matter contents* varied highly and increased from values around 20–30 mg l^{-1} at the sea side to around 400–500 mg l^{-1} at inner compartments (Fig. 4). Highest values were found where the river Ems enters the Ems-Dollard area.

Light attenuation coefficients K_d varied from roughly 0.5 m^{-1} (at the seaward station 1) to values above 10 m^{-1} at stations 4–6 (Fig. 4, appendix D Fig. D3). Since K_d depends on wind conditions, especially in shallow areas, all measured values were snapshots (Table 3). As for suspended matter, at station 4 (just there where the Ems rivers enters the Ems-Dollard area) values generally were highest.

Nutrient concentrations (summarized in Table 3, and level plots in Fig. D2, appendix D) showed a standard pattern throughout the year for this part of the world: low concentrations of ortho-P and silicate were found in spring (in this sequence) as a result of algae uptake. Nitrate concentrations were lowest in (early) summer. For ammonium, values were highest in winter months, due to a low biochemical oxidation rate (Lohse et al., 1993; Herbert, 1999; Zheng et al., 2017).

Oxygen saturation (Fig. 5) usually was around 100%, and just a bit lower at sites 4 and 5. Oxygen concentrations usually drop to lower values in deeper areas as illustrate for the Ems-river by Talke and De Swart (2011), but for the estuary, no additional data were available.

Chlorophyll-a concentrations fluctuated between 2 and 5 µg l^{-1} in winter periods and 40 µg l^{-1} during blooms (Fig. 5). Highest concentrations were found around day 120 in 2013 at station 2 and somewhat earlier in 2012 (Spring bloom) for stations 1–3. At the inner stations, chlorophyll-a concentrations were lowest.

4.2. Photosynthetic parameters

The steepness of the production curve is represented by α^B (Fig. 6 and Fig. 7). Minimum values for α^B varied between 0.007 (station 6) and 0.018 (station 4) mg C (mg chla)$^{-1}$ h^{-1} (µE m^{-2} s^{-1})$^{-1}$. (See Table A2 (appendix A) for conversion to values in mg C (mg chla)$^{-1}$ (E m^{-2})$^{-1}$ -units.) Maximum values were three exceptional values of 0.8 (station 1, 16 Feb 2012) and 0.26 and 0.27 (station 4, 18 Jul 2013 and 14 Nov 2013), respectively. The mean value for α^B for all stations (excluding the extreme outlier of 0.8) was 0.049 ± 0.031 mg C (mg chla)$^{-1}$ h^{-1} (µE m^{-2} s^{-1})$^{-1}$. There is some variation in the values of α^B between stations, with station 4 having the highest values for most of the year (Fig. 6 and Fig. 7). Seasonality is not very obvious for most stations except for station 4; here values in winter are lower than in the other seasons. The spread around the median value is also largest at station 4 (Fig. 7).

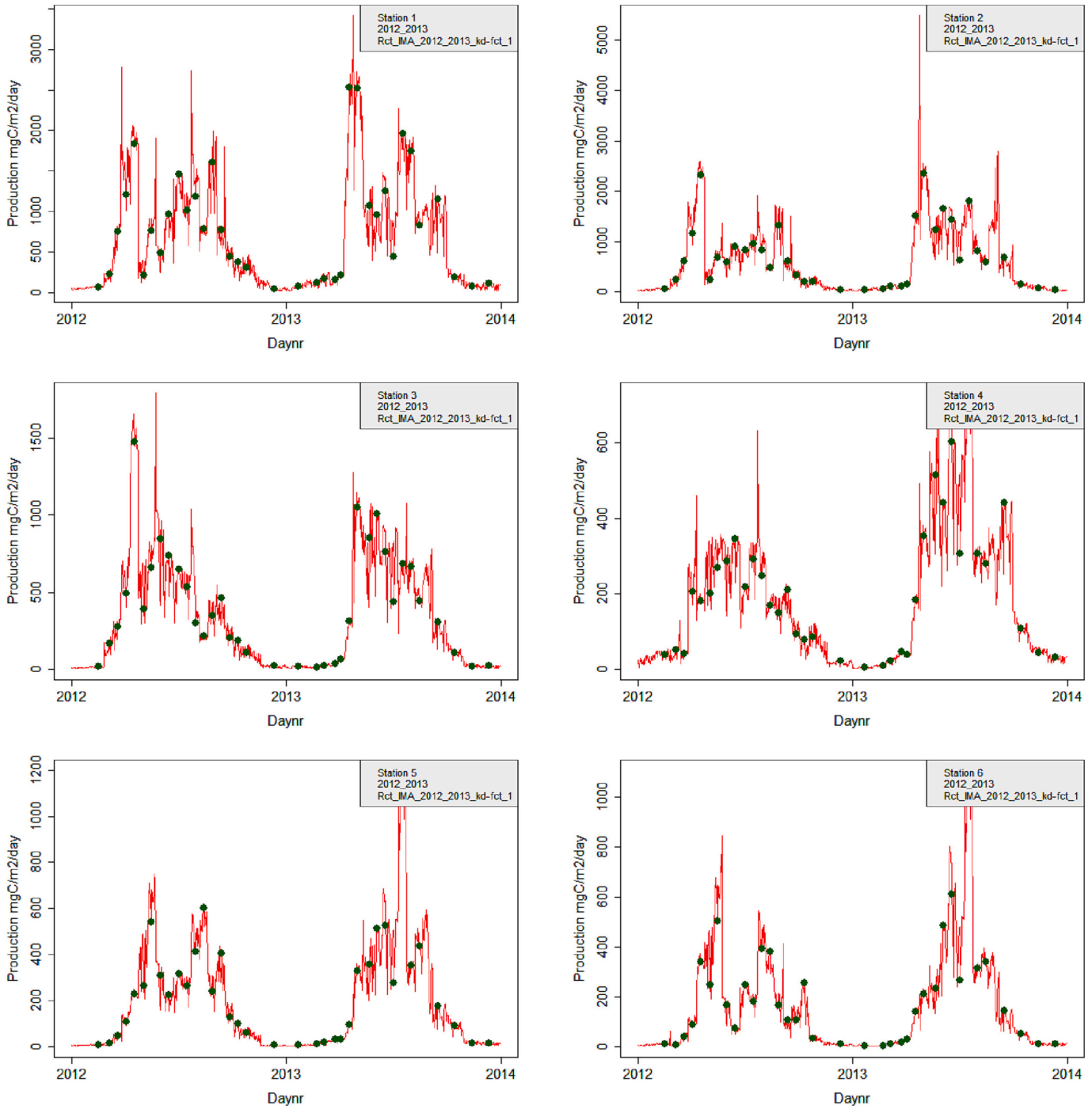

Fig. 10. Computed gross primary pelagic production (mg C m^{-2} day^{-1}) for each station in 2012 and 2013, based on the derived photosynthetic parameters, observed and interpolated chlorophyll-a values, extinction coefficients and temperatures plus actual solar radiation available on an hourly basis. Situation for the channels at high water. Scales differ per station. "Rct_IMA_2012_2013_kd-fct_1" is a code used for the analysis.

The mean maximum productivity P^B_{max} ranged between 4.9 ± 3.0 mg C (mg chla)$^{-1}$ h^{-1} (station 6) and 6.4 ± 3.5 mg C (mg chla)$^{-1}$ h^{-1} (station 3). Minimum values were 1.1 (station 5) and 1.4 (station 1 and 2) and maximum value reached 22.2 (station 3) and 19.6 mg C (mg chla)$^{-1}$ h^{-1} (station 2) (Fig. D4, appendix D). In 2012, the highest P^B_{max} values for stations 1 and 2 were reached in summer around day 250, and earlier (day 180–200) at stations 5 and 6. For stations 3 and 4 there is no clear seasonal pattern. In 2013, the maximum values for all stations are around day 180–200, thus earlier than in 2012 for stations 1 and 2 (Fig. 6, Fig. D4 in appendix D).

4.3. Effects of temperature and nutrients

The steepness of the P—I curve (α^B) is supposed to be independent of temperature, which is confirmed in this study (Fig. C2). The maximum productivity P^B_{max} shows a positive relationship with temperature for the inner (stations 5 ± 6) and mid (station 3 ± 4) regions, but for the outer stations (1 ± 2) this relationship shows a dip around 15 °C (Fig. 8). Closer examination of the nutrient concentrations revealed that the lack of a relation between P^B_{max} and temperature occurred in April–May and coincided with low concentrations of Si, ortho-P as well as N (Fig. 9). The dashed line connecting maximum values of P^B_{max} vs T is included,

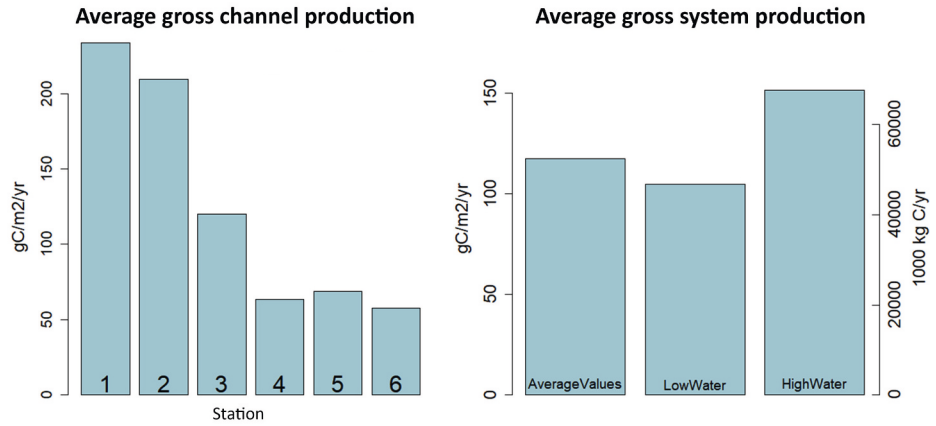

Fig. 11. Left: Averaged (2012−2013) gross primary production for each channel station (g C m^{-2} y^{-1}), at average water level. Right: whole system production for 2012–2013 in average, low water and high water, per m^2 (left axis) and as total (right axis).

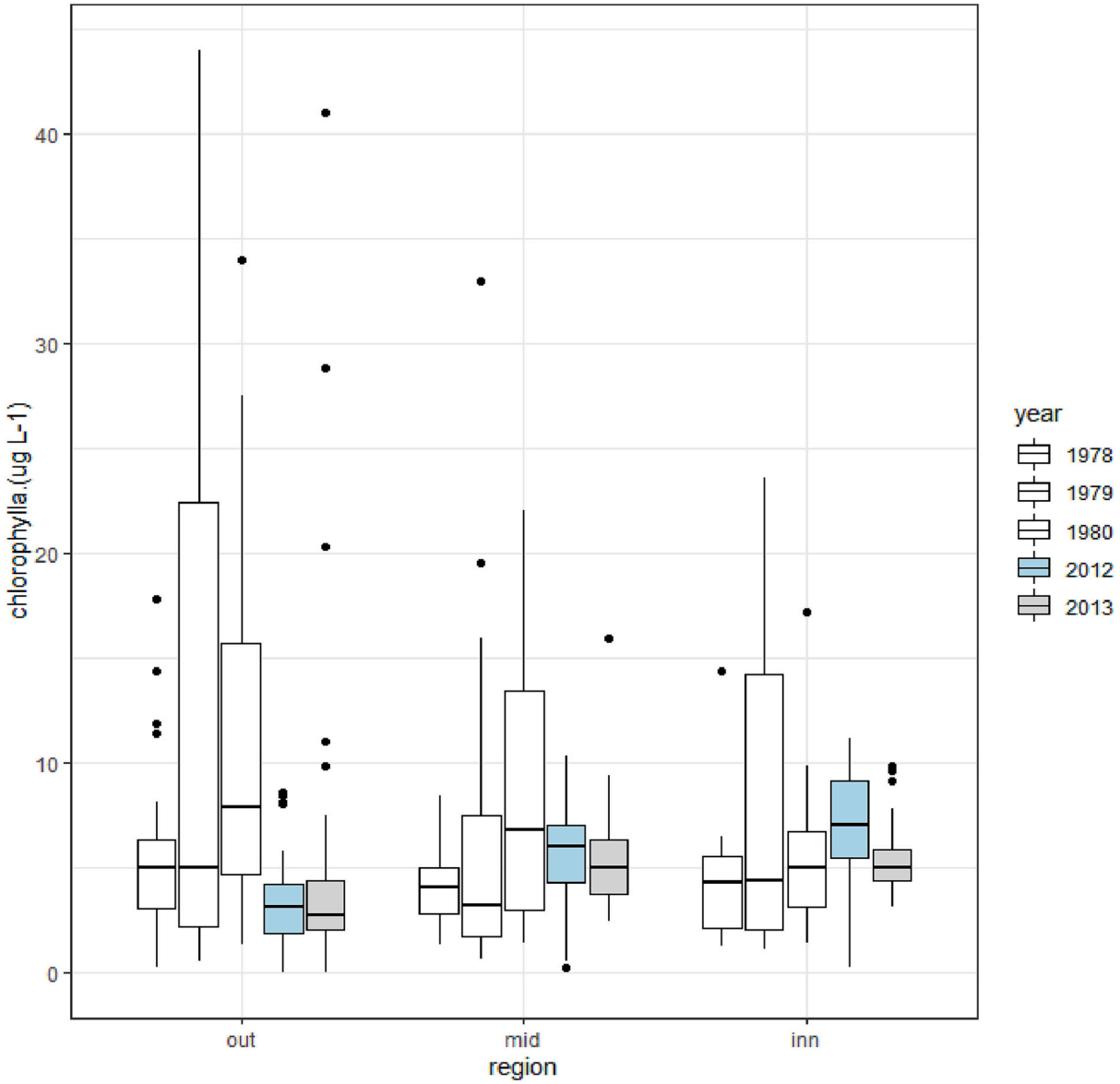

Fig. 12. The year-averaged chlorophyll-a concentration in the years 1978–1979-1980 and 2012–2013 in the outer (out), mid and inner (inn) regions of the Ems-Dollard estuary.

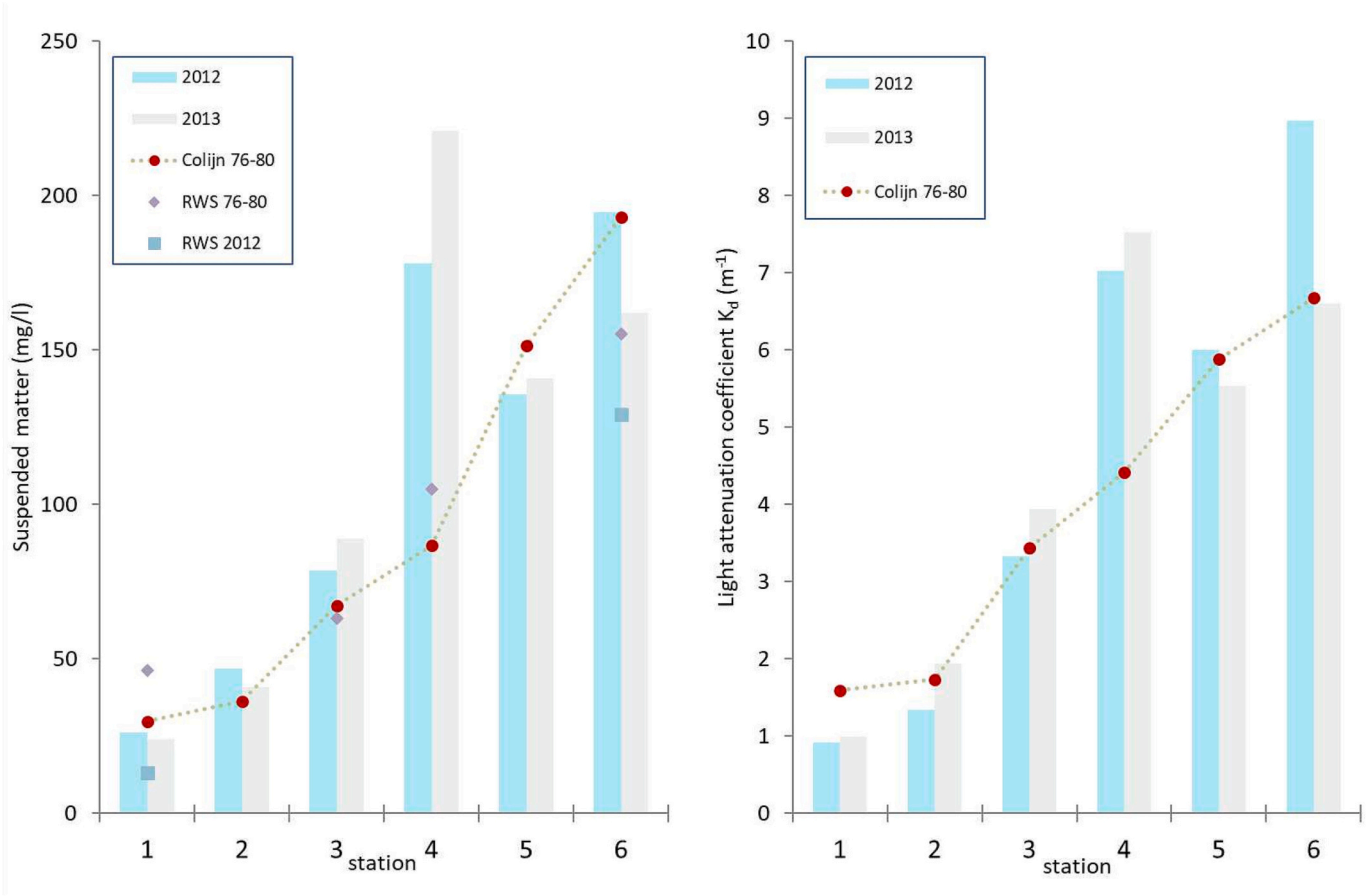

Fig. 13. Averages of suspended matter concentrations (left) and of the light attenuation coefficient (K_d) at all six stations, and averaged data by Colijn (1983) and from Rijkswaterstaat monitoring in 1976–1980 (suspended solids only). Rijkswaterstaat monitoring only covered a few sites.

and where deviations from this line are most obvious, low concentrations all nutrients were observed, supporting the idea of an existing nutrient co-limitation during the April–May months. Furthermore, P^B_{max} as function of temperature shows a significant variation, but next to the nutrient shortage at stations 1 and 2, no explanation could be found. Possible effects of phytoplankton species on P^B_{max} and α^B could not be analysed properly because of the too large variability of algae groups present in the system.

The light intensity I_{max} at which P^B_{max} is found also shows a positive relationship with temperature (appendix C, Fig. C2).

4.4. System primary production

The maximum calculated gross pelagic primary production per day ranged from 2500 mg C m^{-2} for station 1 and 2, to 600–1000 mg C m^{-2} for the other stations (Fig. 10). These maximum daily production rates are earlier in the year for stations 1–3 compared to stations 4–6 (Fig. 10). Yearly gross primary pelagic production values at average high water decrease from station 1 towards stations 4, with a roughly equal production for stations 4,5 and 6 (Fig. 11, left). Taking low- and highwater on the tidal flats and in the channels in compartment 1–6 into account, as well as the size of each compartment, the gross primary production for the whole estuary was computed (Fig. 11, right).

Details for production are in Fig. D4 and Fig. D5 (appendix D), as are total production results per compartment. Some extra details are outlined in appendix D, Fig. D6.

5. Discussion

5.1. State variables

Chlorophyll-a concentrations as reported in this study (Fig. 5) are comparable to other coastal areas in the Netherlands. For the western Wadden Sea, Beukema et al. (2002) reported year-averages around 8 μg chla l^{-1} for the 1980–2002 period at high water near the island of Texel. Kromkamp and Van Engeland (2010) reported year-average values of around 7 μg chla l^{-1} at the sea side of the Western Scheldt area in the southern part of the Netherlands for the 1985–2005 period. Very few papers report year-average chla-values, since most publications focus on (average) summer values. An analysis (Brinkman, 2008) of the monthly RWS-monitoring data for the site Zuidoost-Lauwers (just west of Huibert Gat, see Fig. 1) showed summer-average values between 16 and 18 μg chla l^{-1}, with averages values of around 20 μg chla l^{-1} for the April–September period and average maximum of values 35–40 μg chla l^{-1}; thus similar to the values reported in the current study (Fig. 5).

To compare the chlorophyll-a concentrations found in this study with the concentrations reported in Colijn (1983) for the 1978–1980-period, the site data were grouped to outer, mid and inner region (Fig. 12). While variations in the chlorophyll-a concentrations are high especially for the data from Colijn, the median concentrations are lower in 2012 and 2013 compared to 1978–1980 for the outwards stations (1 and 2), and comparable for the inner stations (5 and 6) except for 2012 when concentrations were higher. This reflects the overall system changes: finishing discharges of potato starch and straw-board industry waste water, plus a decreased eutrophication and thus lower contents of phosphorus and nitrate in the outer region (Fig. B1, appendix B).

Suspended matter values reported by Colijn (1982) are plotted in

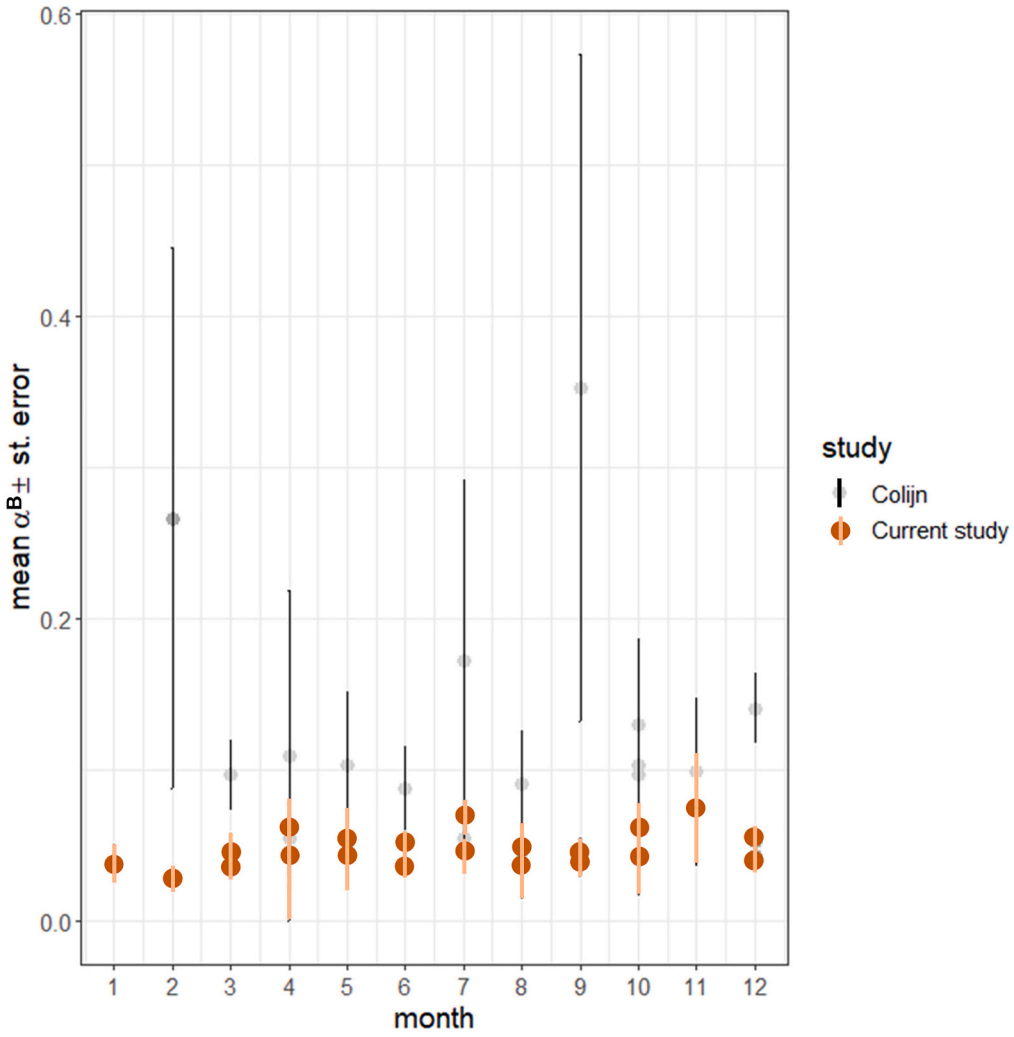

Fig. 14. Mean values per month for α^B (mg C (mg chla)$^{-1}$ h^{-1} (µE m^{-2} s^{-1})$^{-1}$) by Colijn (1983) and in the current study. Note the high standard error for the values reported by Colijn.

Fig. 13. Especially at station 3 and 4, 2012–2013 values are considerably higher (125 and 230% respectively) than the 1978–1980 values. Stations 1 and 2 are mainly influenced by North Sea water while stations 5 and 6 mainly reflect local processes (sedimentation and resuspension of silt and sand). Conditions at stations 3 and 4 can be considered to be partly influenced by the sea, but predominantly by input from the river Ems. Using salinity as a proxy for sea and river input, no change in salinity and thus the ratio between river-sea water input could be detected. In the Dollard area itself with its standard high suspended silt content, differences are about 9% lower in 2012–2013, which is considered as not being significantly different.

Compared to the 1978–1980 results by Colijn (1982) it must be concluded that in the outer area (stations 1) the light attenuation coefficients K_d values (0.95 m^{-1}) are lower than the K_d reported by Colijn (1.59 m^{-1}) (Fig. 1313). For all other stations, the values in the present study are similar or higher than those reported by Colijn: station 2 (1.63 vs 1.73 m^{-1}), 3 (3.62 vs 3.44 m^{-1}), 4 (7.26 vs 4.41 m^{-1}), 5 (5.77 vs 5.88 m^{-1}) and 6 (7.82 vs 6.67 m^{-1}). The differences are most pronounced at station 4.

5.2. Photosynthetic parameters

5.2.1. Photosynthetic parameter α^B

Values for α^B ranged in our study between 0.006 and 0.26 mg C (mg chla)$^{-1}$ h^{-1} (µE m^{-2} s^{-1})$^{-1}$ with the value of 0.80 at station 1, February 2012, considered as an outlier. Various authors consider 0.11 mg C (mg chla)$^{-1}$ h^{-1}(µE m^{-2} s^{-1})$^{-1}$ to be the theoretical maximum value for α^B (Bouman et al., 2018; Platt and Jassby, 1976; Falkowski, 1981; Lohrenz et al., 1994). In the current study, values higher than this maximum were recorded on 4 occasions (including the outlier). Other studies have also reported higher values than 0.11 for α^B (for the Wadden Sea area: Loebl et al., 2007; Jacobs et al., 2020). Generally, high values for α^B are related to low chlorophyll-a concentrations. However, in the current study the chlorophyll-a concentrations were not exceptionally low (Fig. 5). The extreme α^B-value of 0.8 could also be the result of an erroneous light measurement inside the incubator flask. In addition, the use of GF/F filters, with a 0.7 µm effective pore size, could result in loss of the smallest phytoplankton fraction, e.g. cyanobacteria. A small loss at times when the contribution of this group to the total chlorophyll-a concentration is relatively large might also result in higher values for α^B.

The other three high values (0.19, 0.26 and 0.27) are all at station 4, where turbidity is highest as well.

Tillmann et al. (2000) found a range of 0.007 to 0.039 mg C (mg chla)$^{-1}$ h^{-1} (µE m^{-2} s^{-1})$^{-1}$ for α^B at the Büsum Mole (a site in the German Wadden Sea, Schleswig-Holstein), values well below our highest values.

The values Colijn (1983) presented for the Ems-Dollard area were occasionally high as well with maximum values of 0.36, 0.17 and 0.14 mg C (mg chla)$^{-1}$ h^{-1} (µE m^{-2} s^{-1})$^{-1}$. Colijns minimum value (Colijn, 1983) was 0.042 mg C (mg chla)$^{-1}$ h^{-1} (µE m^{-2} s^{-1})$^{-1}$; almost 50% of

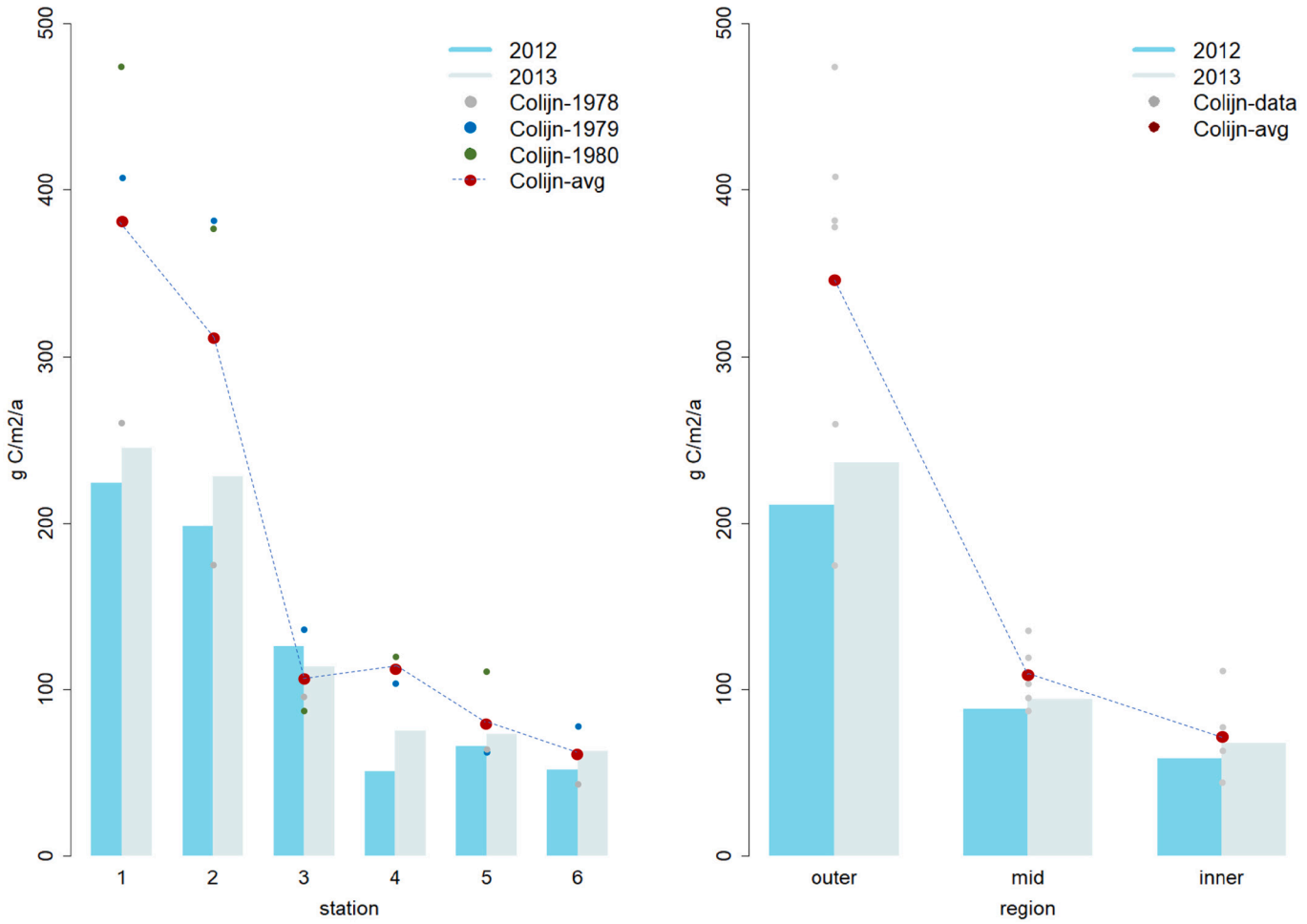

Fig. 15. Annual gross primary production for each station (left) and the three regions as used by Colijn (average of the two stations within each region), plus the values for 1978–1979-1980 from Colijn (1983) (dots). Red dots denote averages per station (left) and per region (right). (For interpretation of the references to colour in this figure legend, the reader is referred to the web version of this article.)

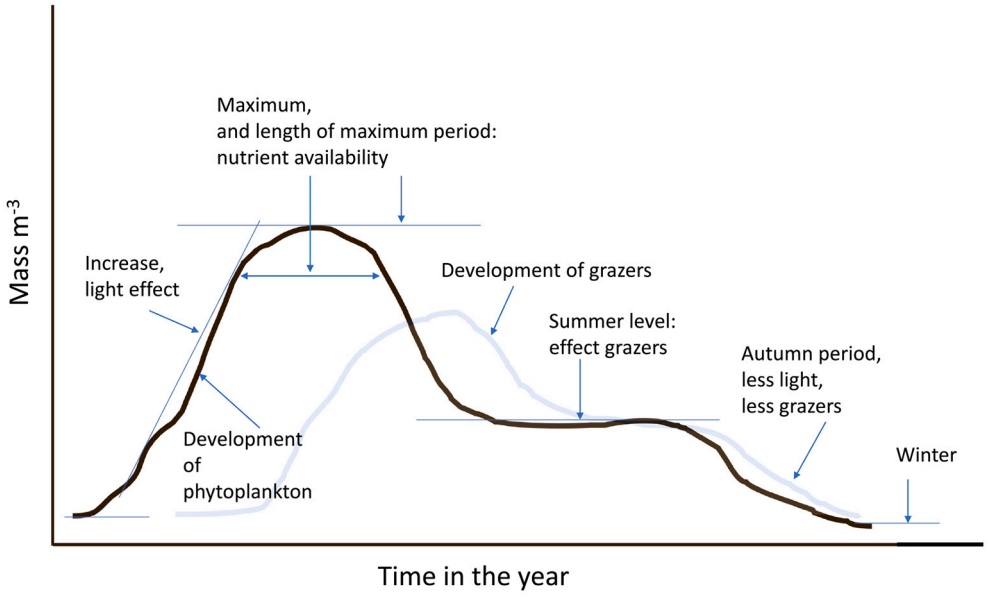

Fig. 16. Simplified development of phytoplankton and grazers in a system, illustrating when availability or presence of light, nutrients and grazing may become limiting.

our values are below that value. The mean values for α^B per month in the current study were always lower than the mean α^B reported by Colijn (1983) (Fig. 14).

Values for α^B in the current study showed seasonal variability. In 2012, highest values were found at the end of winter/ the beginning of spring (station 1 and 3), in autumn (station 1 and 2) or summer (station 4) (Fig. 1). High values in spring and autumn for α^B correspond to a general pattern reported for temperate coastal regions (Sathyendranath et al., 1995; Bode and Varela, 1998). The high values for α^B in spring and low values in summer may be explained by adaptations of the phytoplankton community to increasing radiation in spring and constant high radiation in summer (Bode and Varela, 1998). In 2013 there is no clear seasonal pattern (stations 1–3 and 5–6) but high values of α^B in July and the end of November 2013 at station 4.

The value of α^B is said not be related to temperature, but previous studies have found mixed results, with variations in α^B being both independent (Post et al., 1985) and dependent on water temperature (Lohrenz et al., 1994). In the present research, we could not detect a temperature dependency. Estimates for α^B have also been correlated with irradiance (or irradiance average of three previous days) (Platt and Jassby, 1976); in the current study this dependency was not analysed.

Behrenfeld et al. (2004), Claquin et al. (2010) and Mangoni et al. (2009) state that photosynthetic parameters are higher in the absence of nutrient stress and that α^B increases when light is limited (Behrenfeld et al., 2004; Falkowski and Raven, 1997). In the UK-coast, despite high SPM concentrations, α^B remained low from April to August suggesting a weak photo-acclimation by phytoplankton. Moreover, α^B and DIN concentrations showed a similar pattern along the year in the UK-coast (Napoléon et al., 2012). Thus, the capacity to respond to changing light in the north of the transect in spring and summer might be affected by the nutrient stress, and, if the case, being consistent with the results showed by Behrenfeld et al. (2004) and Claquin et al. (2010).

This would imply that at the inner stations (relatively low light conditions without nutrient stress) α^B should show higher values than at both outer stations. In the Ems-Dollard area, nutrient stress is not present, except for a short period at the outer station(s). However, even when considering stations 1 and 2 alone, the only two stations showing a shortage of nutrients in months April and May, a relationship of α^B with nutrient concentrations was not detected. The aforementioned relationship of α with turbidity does not seem to hold in the Ems-Dollard area: despite higher turbidities now for most stations, we found lower α^B -values compared to the 1976–1980-period.

Tillmann et al. (2000) showed for 10 diatom culture systems that α^B-values differed from 0.01 to almost 0.025 mg C (mg chla)$^{-1}$ h^{-1} (μE m^{-2} s^{-1})$^{-1}$. Variations in the value of α^B might thus also be related to changes in species composition (Côté and Platt, 1983). In our case, phytoplankton data were too varying, and the number of observations too low, to detect any relationship of α^B with phytoplankton species composition.

5.2.2. Photosynthetic parameter P^B_{max}

Values for P^B_{max} were within the theoretical range of 0.2 and 25 mg C (mg chla) $^{-1}$ h^{-1} (Bouman et al., 2018; Platt and Jassby, 1976; Falkowski, 1981; Lohrenz et al., 1994). For 1978–1980, Colijn (1983) reported values for P^B_{max} ranging between 4.1 and 50 mg C (mg chla) $^{-1}$ h^{-1}, although all his high values (>12 mg C (mg chla) $^{-1}$ h^{-1}) had large uncertainties. Tillmann et al. (2000) arrived at a maximum values of 10 mg C (mg chla) $^{-1}$ h^{-1} for the Büsum Mole in 1995–1996. These authors also examined 10 diatom cultures and found P^B_{max} -values ranging from 3 to almost 8 mg C (mg chla) $^{-1}$ h^{-1}.

In the current study, the highest values for P^B_{max} were found in summer for all stations and in both years which is in line with other studies (Sathyendranath et al., 1995; Sakshaug et al., 1997; Bode and Varela, 1998). The seasonal effect could be due to a relation of P^B_{max} with temperature as reported in other studies (e.g. Platt and Jassby, 1976; Lohrenz et al., 1994).

Bouman et al. (2005) also recorded differences in the correlation between temperature and P^B_{max} between regions and hypothesized that the lack of such a relation might be due to the negative correlation between nutrients (nitrate) and temperature, in other words, in those systems P^B_{max} is limited by the available nutrients in the water. In the current study, P^B_{max} might also be depressed at temperatures >10 °C due to low nutrient concentrations, but rather than reported by Bouman et al. (2005) there might be a combined effect of P, N and Si (for diatoms) limitation (Fig. 9).

5.2.3. Photosynthetic parameter I_{max}

The light intensity at which P^B_{max} was found increased with temperature; the range of 70–700 μE m^2 s^{-1} (530 averaged) found is not very different from Colijns results (150–630 μE m^{-2} s^{-1}, 365 averaged). Lampert and Sommer (1993) mention circa 200–1000 μE m^{-2} s^{-1} as usual range for I_{max}; about 15% of our values are below this range, and none above. Colijns values were all within this range.

5.3. System production

5.3.1. Vertical mixing

For calculation of primary production at each station chlorophyll-a concentrations and temperatures were assumed constant over depth. Vertical profiles were not measured in this study, and although it has been shown that gradients in temperature, chlorophyll-a and suspended solids can occur under calm weather conditions (*in* Brinkman et al., 2014), we think that it is justified to assume a vertically well-mixed situation since the average wind velocity in the Ems-Dollard areas is 7 m s^{-1} (KNMI, 2021). Suspended solid concentrations will increase with depth for most weather conditions. But, as a result of the relatively high light attenuation values, only the upper part of the water column is important for the gross primary production, and higher concentrations of suspended matter in deeper parts of the system will have only a minor effect on our results.

5.3.2. Gross pelagic primary production

Unfortunately, despite many data on chlorophyll-a, integral gross pelagic primary production values for the Wadden Sea area are scarce. In most cases, values for single stations are available. Cadée and Hegeman (1974) came to maximum values of 3000 mg C m^{-2} d^{-1} for the Marsdiep area (the western-most area of the Dutch Wadden Sea) in 1974. It should be noted that sampling always took place at high water, therefore representing the North Sea coastal water rather than the Wadden Sea. Tillmann et al. (2000) reported maximum values of 2000 mg C m^{-2} d^{-1} for the Büsum Mole (Schleswig-Holstein, Germany) in 1995–1996.

Colijn (1983) calculated daily production values up to about 6000 mg C m^{-2} d^{-1} for the most productive outer areas, mostly in early summer 1979 and 1980, which is definitely higher than the maximum values of about 3000 mg C m^{-2} d^{-1} found in the current research (Fig. 10).

Annual gross pelagic primary production was reported between 200 and 400 g C m^{-2} y^{-1} for the Marsdiep area based on chlorophyll-a and solar radiation data for the period 1980–1992 (Bot and Colijn, 1996) and somewhat higher (between 300 and 400 g C m^{-2} y^{-1}) for the same site and same period (Cadée and Hegeman, 1993) albeit based on a somewhat different procedure (Cadée and Hegeman, 1974). Thus, these production estimates are considerably higher than the values of 200–220 g C m^{-2} y^{-1} found for both outer Ems-Dollard stations in 2012 and 2013. But at Büsum Mole, also a seaward station as part of the German Wadden Sea Tillmann et al. (2000) arrived at an annual gross production of 124 (1995) and 176 (1996) g C m^{-2} y^{-1}.

The whole Ems-Dollard system production of about 120 g C m^{-2} y^{-1} (Fig. 9, right) is mainly determined by areas 1 and 2 (with stations 1 and 2, Fig. 1), a result of the highest production per m^2 and of the large size of these areas. The lower gross primary production per m^2 at the inner stations (Fig. 9, right) is caused by their much higher turbidity status.

For the Sylt-Rømø area (the Wadden Sea part on the German-Danish border), Asmus et al. (1998) found 101–140 g C m^{-2} y^{-1} for the Königshaven area (a part of the larger Sylt-Rømø Wadden Sea area), and estimated for the whole basin, which is deeper, 160 g C m^{-2} y^{-1} as annual gross production. The Sylt- Rømø area is less turbid than the Ems-Dollard and has a much lower fresh water inflow and consequently a lower nutrient supply.

Fig. 15 illustrates the differences between the present gross primary production rates and those from Colijn (1983), for each sampling station and, conform Colijn, grouped into an outer (Fig. 1, area 1 and 2), mid (3 and 4) and inner region (5 and 6). In the highest productive outer region, production decreased most, causing an overall lower primary production. It underlines the importance of this outer region as supplier of food for the whole area. This reduction most probably is nutrient steered since nutrient concentrations during the phytoplankton bloom period drops to low values. At stations 3–6, nutrient concentrations stay at a (much) higher level, and light is the limiting factor. Especially at station 4, where the river Ems enters the main estuary, the difference between the Colijn-period and our 2012–2013 results is striking. It is this station where turbidity increased most (230%), as well as suspended solid contents and light attenuation levels (Fig. 13).

In estuarine systems, concentrations of suspended solids can be high. The inner parts usually are silty as a result of transport from rivers and the sea (Postma, 1961; Groen, 1967; Wang et al., 2018) and as a result of dredging activities to deepen harbours, rivers and channels. Dredging activities are important in the area (Van Maren et al., 2016), with over 10 million m^3 y^{-1} are dredged from inner compartments. Dredged material is mostly transported to sites near the Ems-harbour (Fig. 1) within the estuary, resulting in a transport of the sludge back to the inner parts by the tides. Since the end of the 1970's, the amount of sludge dredged and transported hardly changed (Van Maren et al., 2016). Deepening of the channel near the Emden harbour as well as the increased depth of the Ems-river to allow large ships sail from the Meyer shipyard in Papenburg seawards caused a drastic increase in suspended solid concentrations, not only near the Emden harbour, but also upstream the Ems river, up to surface concentration of 1000 mg l^{-1} (Schuttelaars et al., 2013; De Jonge et al., 2014). Consequently, it is near site 4, where the Ems river enters the Ems-Dollard area, where the highest increase in suspended solid levels is observed and, as a result, a substantial reduction in primary production takes place.

An important aspect not mentioned so far concerns effects of higher trophic levels on the gross primary production. In management documents, nutrients often are depicted as the main steering factors for chlorophyll-a concentrations and primary production. However, a large and active population of grazers will highly affect phytoplankton (and thus chlorophyll-a) concentrations and turnover rates, and by that even reduce a possible nutrient deficiency. In a grazer-controlled system (or period), chlorophyll-a concentrations will become more and more independent from nutrient concentrations. Such a situation will not occur throughout the year, but most pronounced after the spring bloom and depends on the development rate of grazers which will be different depending whether it concerns zooplankton (fast) or zoobenthos like shellfish (occurs mostly in summer and takes longer to develop). We sketched such a characteristic picture of nutrients, phytoplankton and grazers in Fig. 16. However, reliable data on grazing activities are lacking in the Ems-Dollard system, and thus cannot help to understand the differences between the 2012–2013 period and the late seventies (Fig. 15). What is known is that in the mid and inner compartments benthic grazers as Blue Mussels (*Mytilus edulis*) and Common Cockles (*Cerastoderma edule*) are almost completely absent (Van den Ende et al., 2012; Van Asch et al., 2015; Compton et al., 2013), implying that low production values there can only be attributed to high turbidity values.

6. Conclusion

The Ems-Dollard estuary is, like any estuary, a system with relatively clear water at the sea side, and very turbid water in the inner side. Partly, since the 1970's, water quality has improved a lot since organic waste water discharges have disappeared almost completely. Oxygen concentration at the surface of the estuarine water is close to saturation. Also, concentrations of dissolved nutrients decreased a lot, especially the concentrations of ortho-phosphorus and nitrate (both over 50% at station 1, Huibert Gat Oost). However, several man-made changes such as deepening channel parts and thus constantly maintaining an un-natural morphologic system, cause extreme turbidity in parts of the system with, among others, a very light limited and low gross primary production as a result. At the sea-side of the estuary, primary production is similar to what can be found at other sites in the Dutch or German Wadden Sea, and much lower now than thirty years ago. At the inner sides, gross pelagic primary production is low, also somewhat lower than thirty years ago. Together with high contents of suspended silt, unfavourable conditions for grazers might exist. The most turbid area is found there where the Ems-river enters the main part of the estuary, a result of the extremely high contents of suspended matter in the river itself.

Declaration of Competing Interest

Regarding the manuscript entitled "Gross pelagic primary production in the Ems-Dollard estuary" by dr. ir. A.G. Brinkman and dr. ir. P. Jacobs, we both declare that there are no conflicts of interest. Also, there are no directly related manuscripts or abstracts, published or unpublished, by both authors of this paper.

Data availability

Data are available upon request, but these are distributed in many separate files. Takes a lot of time for sharing.

Acknowledgements

Many people contributed to this study. First and foremost, we thank dr. Roel Riegman (IMARES, now Wageningen Marine Research) who was the leading scientist for this study. Field and laboratory work was executed by former colleagues from IMARES, especially Catherine Beauchemin, Susanne Kühn, André Meijboom, Hans Verdaat and Erika Koelemij.

Furthermore, we are grateful to Rijkswaterstaat for their cooperation, with special thanks to the crew of the research vessels Asterias and Kennemer, the monitoring staff and the nutrient lab and Charlotte Schmidt (RWS) who followed the study closely. The Royal Netherlands Institute for Sea Research for allowing the use of their radioisotope laboratory facilities. The Niedersächsischer Landesbetrieb für Wasserwirtschaft, Küsten- und Naturschutz (NLWKN), the Waterschap Hunze en Aa and the Hoogheemraadschap Noorderzijlvest for the use of nutrient data.

Finally, we thank two anonymous reviewers for their valuable remarks.

Funding

The study was commissioned by Rijkswaterstaat (RWS, part of the Dutch Ministry of Infrastructure and Water Management), as part of the research project "Onderzoek Slibhuishouding Eems-Dollard" (Research on mud dynamics in the Ems-Dollard), where Deltares and IMARES (the predecessor of Wageningen Marine Research) co-participated.

Appendix A. Sampling times, variables, parameters, units

Table A1
Dates of visits and whether nutrient sampling (N) and/or ^{14}C-incubations (C) took place. Not all sampling or ^{14}C-incubations could be completed successfully for all visits.

Date/Site	Nutrient analysis						^{14}C-incubations					
	1	2	3	4	5	6	1	2	3	4	5	6
2012-02-16									C		C	C
2012-03-06	N	N	N	N	N	N	C	C	C	C	C	C
2012-03-20	N	N	N	N	N	N	C	C	C	C	C	C
2012-04-03	N	N	N	N	N	N	C	C	C	C	C	C
2012-04-17	N	N	N	N	N	N	C	C	C	C	C	C
2012-05-03	N	N	N	N	N	N	C	C	C	C	C	C
2012-05-15	N	N	N	N	N	N	C	C	C	C	C	C
2012-06-01	N	N	N	N	N	N	C	C	C	C	C	C
2012-06-14	N	N	N	N	N	N	C	C	C	C	C	C
2012-07-02	N	N	N	N	N	N	C	C	C	C	C	C
2012-07-16	N	N	N	N	N	N	C	C	C	C	C	C
2012-07-31	N	N	N	N	N	N	C	C	C	C	C	C
2012-08-13	N	N	N	N	N	N	C	C	C	C	C	C
2012-08-28	N	N	N	N	N	N	C	C	C	C	C	C
2012-09-12	N	N	N	N	N	N	C	C	C	C	C	C
2012-09-26	N	N	N	N	N	N	C	C	C	C	C	C
2012-10-11	N	N	N	N	N	N	C	C	C	C	C	C
2012-10-25	N	N	N	N	N	N	C	C	C	C	C	C
2012-11-29	N	N	N	N	N	N						
2012-12-11	N	N	N	N	N	N	C	C	C	C	C	C
2013-01-22	N	N	N	N			C	C	C	C		
2013-02-21	N	N	N	N	N	N	C	C	C	C	C	C
2013-03-07	N	N	N	N	N	N	C	C	C	C	C	C
2013-03-25	N	N	N	N	N	N	C	C	C	C	C	C
2013-04-04	N	N	N	N	N	N	C	C	C	C	C	C
2013-04-18	N	N	N	N	N	N	C	C	C	C	C	C
2013-05-02	N	N	N	N	N	N	C	C	C	C	C	C
2013-05-22	N	N	N	N	N	N	C	C	C	C	C	C
2013-06-04	N	N	N	N	N	N	C	C	C	C	C	C
2013-06-19	N	N	N	N	N	N	C	C	C	C	C	C
2013-07-03	N	N	N	N	N	N	C	C	C	C	C	C
2013-07-17	N	N	N	N	N	N	C	C	C	C	C	C
2013-08-01	N	N	N	N	N	N	C	C	C	C	C	C
2013-08-15	N	N	N	N	N	N	C	C	C	C	C	C
2013-08-29	N	N	N	N	N	N						
2013-09-16	N	N	N	N	N	N	C	C	C	C	C	C
2013-10-15	N	N	N	N	N	N	C	C	C	C	C	C
2013–11–14	N	N	N	N	N	N	C	C	C	C	C	C
2013-12-12						N		C	C	C	C	C

Table A2
Units of state variables and parameters.

	Variables and parameters	Mnemonic	Unit
	General		
1	Depth (as quantity)	H	m
2	Depth (as variable)	z	m
3	Area	A	m^2
	Nutrients, solids, temperature		
4	Ortho-phosphate	P	µmol P l^{-1}
5	Nitrate	NO_3^-	µmol N l^{-1}
6	Ammonium	NH_4^+	µmol N l^{-1}
7	Silicate	Si	µmol Si l^{-1}
8	Dissolved inorganic C	DIC	µmol C l^{-1}
9	Oxygen	O_2	mg O_2 l^{-1}
10	Oxygen saturation	O_2_sat	%
11	Chlorophyll-a	chla	µg chla l^{-1}
12	Suspended solids	SS	mg DW l^{-1}
13	Turbidity		FTU
14	Conductivity		mS cm^{-1}
15	Salinity		g kg^{-1}
16	Temperature	Temp	^oC
	Light		
17	Solar radiation	I0	W m^{-2}
18	Photosynthetic active radiation	PAR	W m^{-2}
19	Incubation light	I	uE m^{-2} s^{-1}
	15 - > 16 conversion factor	* 0.5	(−)
	15 - > 17 conversion factor	* 4.76	µE m^{-2} s^{-1} (W m^{-2})$^{-1}$ = µmol J^{-1}
	16 - > 17 conversion factor	* 2.52	µE m^{-2} s^{-1} (W m^{-2})$^{-1}$ = µmol J^{-1}
20	Extinction coefficient	Kd	m^{-1}
	Production		
21	^{14}C-activity (disintegration rate per unit volume)	DPM	Mbq ml^{-1}
22	Carbon fixation rate	CP	mg C l^{-1} h^{-1}
23	Productivity as fie of light	PP(I)	mg C (mg chla)$^{-1}$ h^{-1}
24	Maximum value of PP(I)	P^B_{max}	mg C (mg chla)$^{-1}$ h^{-1}
25	Water column production at each depth	Prod(z)	mg C m^{-3} h^{-1}
26	Water column production	ProdSite	mg C m^{-2} h^{-1}
27	Compartment production	ProdComp	mg C m^{-2} h-1
	Yearly compartment production	ProdCompY	g C m^{-2} y-1
28	Yearly system production	ProdSyst	g C m^{-2} y-1
	Productivity parameters		
29	a	a	
30	b	b	
31	c	c	
32	Steepness of P—I curve incubations	alfa	mg C (mg chla)$^{-1}$ h^{-1} (µmol photons m^{-2} s^{-1})$^{-1}$
	equals	* 1 =	mg C (mg chla)$^{-1}$ h^{-1} (µE m^{-2} s^{-1})$^{-1}$
	or	* 278 =	mg C (mg chla)$^{-1}$ (E m^{-2})$^{-1}$

Appendix B. Eutrophication status

In Fig. B1, data for dissolved inorganic phosphorus, nitrate+nitrite, total-phosphorus and total-nitrogen are summarized for the two main inflowing rivers (Ems, 1987–2016, and Westerwoldse Aa, 1978–2015), the Eems-canal (the main canal from Groningen to Delfzijl, 1978–2015) at Farnsum Bridge, and at Huibert Gat Oost (in the northern part of the estuary, 1971–2014). All sites are mentioned in Fig. 1. Note that the Y-axes differ largely; especially those for the Westerwoldse Aa where concentrations of P and N initially were extremely high. Around 1990 a big drop can be observed for three components, except nitrate+nitrite, which is a consequence of the switch from ammonium as main N-component (the river had very low oxygen concentrations before that time) to nitrate + nitrite.

In the Eems-canal, ortho-P and ($NO_3 + NO_2$) contents declined a bit after 1978, but already were rather low by then. In the Ems-river, the observed concentrations for nitrate+nitrite are similar to those in the Eems-canal at Farnsum Bridge, but total-P concentrations tend to increase a lot. This is to be assigned to the increasing suspended matter content in the water, including silt and humus compounds.

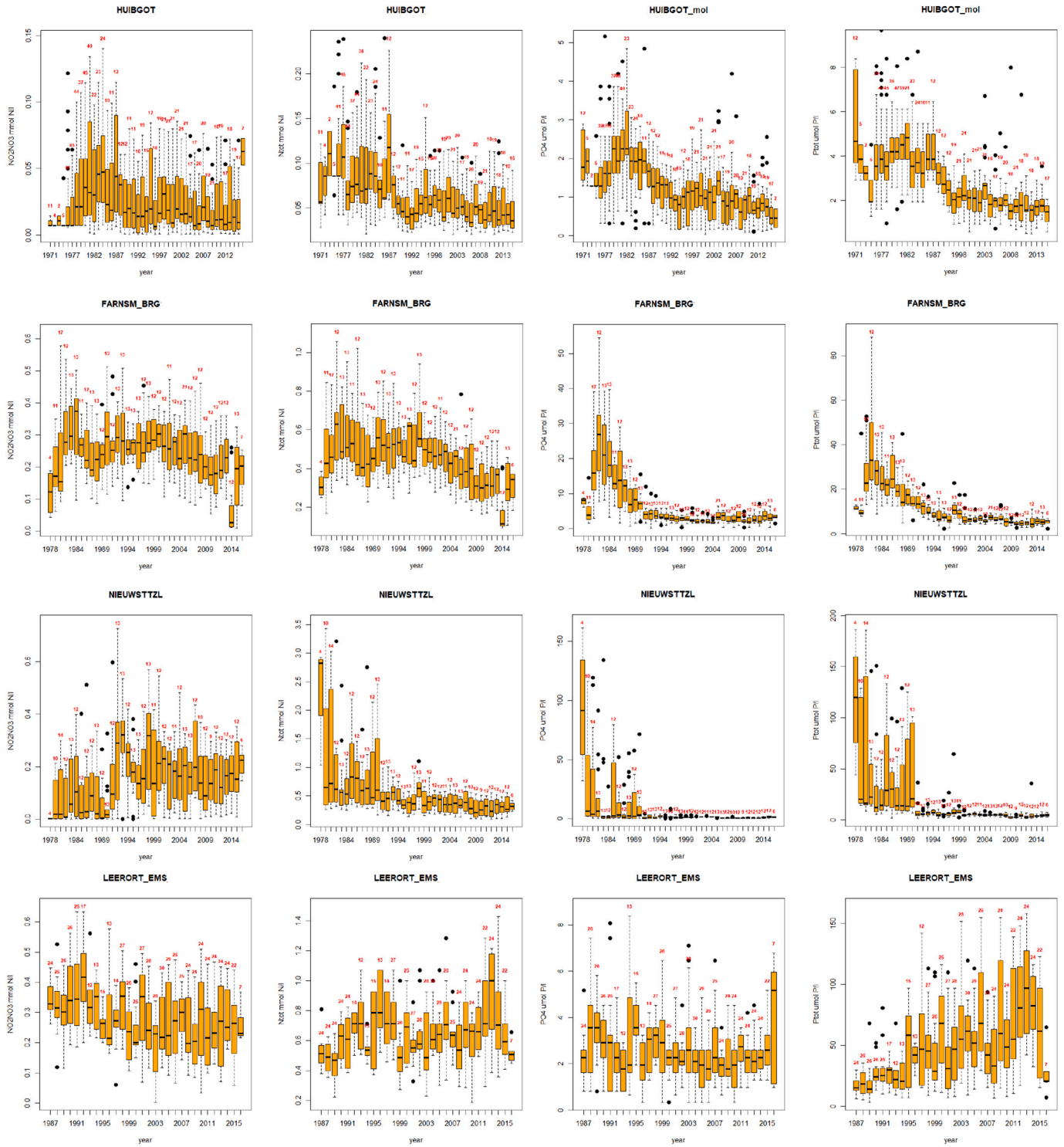

Fig. B1. Concentrations of (nitrate+nitrite), total-N, ortho-phosphate and total-P for Huibert Gat Oost (HUIBGOT, northern estuary part), Farnsum Bridge (FARNSM_BRG, the Eems-canal from Groningen to Delfzijl, and thus the estuary), Nieuwstatenzijl (NIEUWSTTZL, Westerwoldse Aa river) and Ems-river at Leer (LEERORT_EMS). All values in µmol l^{-1}. Note that the sampling periods differ per station. Sampling sites: Fig. 1.
Source: Huibert Gat Oost: RWS, 2017; Farnsum Bridge: Waterschap Noorderzijlvest; Nieuwstatenzijl: Waterschap Hunze en Aa's; Leerort-Ems: Niedersächsischer Landesbetrieb für Wasserwirtschaft, Küsten- und Naturschutz (NLWKN), http://www.wasserdaten.niedersachsen.de/cadenza/pages/map/default/index.xhtml

Appendix C. Analyses

C.1. Analysis of state variables

Nutrients: at each station, 250 ml of water was filtered over 0.45 µm Polydisc filters and stored at 4 °C until further processing by Rijkswaterstaat according to RWS-MWTL analysis procedures (see RWS, 2017). Results are available for dissolved inorganic phosphorus (ortho-P), ammonium (NH_4^+),

nitrate (NO_3^-), nitrite (NO_2^-) and dissolved Si.

Chlorophyll-a: depending on the station, between 50- and 400-ml water sample was filtrated over a GF/F filter (effective pore size 0.7 μm). Samples were taken in duplicate. Filters were wrapped in labelled aluminum foil and kept between −20 and − 80 °C until further processing. Acetone (90%) was added to the filters to extract phytoplankton pigments. Phytoplankton cells on filters were destroyed (using a CO_2-cooled homogeniser with glass beads) to facilitate extraction. Samples were centrifuged and supernatant was analysed using a PAM (Pulse Amplitude Modulation) fluorescence meter. Chlorophyll-a from spinach (Sigma) was used a reference. The method is described in more detail in Holm-Hansen et al. (1965).

Suspended solids: depending on the station, between 400 and 50 ml of water was filtrated over a GF/C pre-weighted filter (effective pore size 1.2 μm). Samples were taken in duplicate. Filters were placed in petri-discs and stored at 4 °C until further processing. Back in the laboratory on Texel the filters were dried (50 °C, min 16 h) and weighted. As control, two filters with reference material were also part of the analysis. The described procedure is in accordance with the MWTL analysis procedure (RWS, 2017).

Conductivity/salinity: measured with an "IntelliCAL"-probe (Hach, 2012a). Salinity is computed by the instrument from the conductivity data.

Oxygen concentration: measured with an IntelliCAL™ LDO101 Rugged Luminescent/Optical Dissolved Oxygen (LDO) meter with a Lumiphore sensor. Sensitivity range 0.05 to 20.00 mg l^{-1} (Hach, 2012b).

Temperature: included with oxygen and conductivity measurements.

C.2. Pocket Box measurements

The PocketBox (4h-Jena Engineering, 2021) was equipped with a couple of sensors, sampling took place by a pressure pump, sampling at 1 m depth. Data were stored every minute.

Conductivity: measured by an AADI 3919A 1 W inductive conductivity sensor, ranging 0–75 mS cm^{-1} (AANDERAA, Norway; http://www.aadi.no).

Oxygen: measured through an AADI 3835 optode sensor (optical fluorescence quenching technique, see e.g. http://en.wikipedia.org/wiki/Optode), ranging from 0 to 500 μmol O_2 l^{-1} ≈ 16 mg O_2 l^{-1}). Manufactured by AANDERAA, Norway (http://www.aadi.no).

Light attenuation: the PocketBox was equipped with two C-Star light attenuation sensors, (WETLabs, Oregon, USA; Wetlabs, 2012), with light paths of 25 and 10 cm, respectively. The light source operates at 470, 530 and 650 nm wavelength. It appeared that in the most turbid regions, even the 10 cm pathway was too long.

Temperature: measured by several sensors. One is separately mounted in the PocketBox, a second sensor is combined with the Optode-oxygen sensor. The type of sensors is not specified.

Coloured dissolved matter (CDOM): measured with a CYCLOPS-7 Submersible Fluorimeter (nr PN 21000–000), manufactured by Turner Designs California, USA, see http://www.turnerdesigns.com/applications/dom-fluorometer-application-notes.

A Yellow Substance sensor is part of the AOA-equipment ("Algae OnlineAnalyser"). It is also a fluorometric analysis and should cover more or less the same components as the CDOM-analyser does.

Next to coloured dissolved organic matter, the CYCLOPS-7 Submersible Fluorometer also measures chlorophyll-a. It is a separate sensor in the PocketBox, measuring range 0–500 μg l^{-1}, lower detection limit 0.025 μg l^{-1}. The fluorometer was in vivo calibrated using *Skeletonema costatum* monocultures. See also http://www.turnerdesigns.com/applications/dom-fluorometer-application-notes.

C.3. Under-water light climate

Vertical light profiles (I_z (μE m^{-2} s^{-1}) versus depth z (m)) were assessed using two Licor underwater quantum sensors (Licor, 2022); one sensor measuring the atmospheric radiation level and the second measuring the light level at each depth. Data were analysed using Lambert-Beer's equation.

$$I_z = I_0 exp(-K_d\, z) \quad \left(\mu \mathrm{E\ m^{-2}\ s^{-1}}\right) \tag{C1}$$

where I_0 is the light intensity right below the water surface and K_d the light attenuation coefficient (m^{-1}). I_0 does not equal solar irradiation I (μE m^{-2} s^{-1}) because of reflection at the surface of about 5–10%, which depends on the solar angle and weather conditions (cloudy or clear sky, see e.g. Kirk, 1994). Also, the position of the underwater measurements close to the water surface is uncertain due to waves. Both phenomena are described by a factor (1-β):

$$I_0 = I \bullet (1-\beta) \quad \left(\mu \mathrm{E\ m^{-2}\ s^{-1}}\right) \tag{C1a}$$

Estimation of K_d, together with β, was performed with a non-linear analysis on the data (I ~ z). The minimum of

$$LSQ = \sum_{z=0}^{z=H} (\hat{I}_z - I_z)^2 \tag{C1b}$$

must be found, with $\hat{I}_z$ as the computed light intensity at each depth z, and H the total depth at that site. By this approach, errors at high values of I_z (close to the surface) are crucial. Although the sensor values have the same absolute error (and thus, the necessary condition of normality of the residues for applying eq. (C1b) is met), large variations appear from time to time, especially with increasing wave height. In eq. (C1), the correct value of I_0 is important. The more usual approach of estimating K_d after a log-transformation of eq. (C1) is sensitive to uncertainties at large depths.

Estimation of K_d and β were performed using R (R Core Team, 2021) and its NLS-routine (Bates and Chambers, 1992). Sometimes errors in I_z for small z (close to the water surface) can be large, and therefore all analyses were also performed after omitting the first 10 and 20 cm-values, respectively. Thus, for each data set, three values for K_d and β are obtained. If these values are not the same for all three data sets, an inspection 'by eye' was done and a best value was selected. An example is presented in Fig. C1 for one measurement at station 6, in the turbid and shallow Dollard-area. Especially in shallow situations where light attenuation is high, omitting the first 10 or 20 cm observations may alter the result for the attenuation coefficient. In more clear and deeper water this effect is less pronounced.

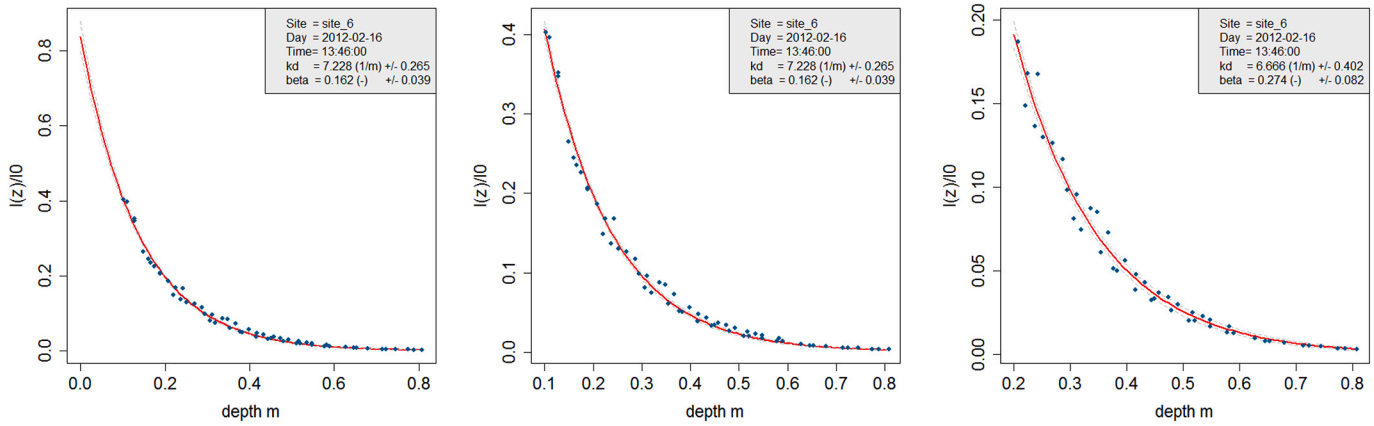

Fig. C1. Under water light climate analysis: three attempts without and with dropping part of the upper water column data. In the middle and right graph, the first 10 and 20 cm, respectively, have been omitted. Both left analyses give 7.23 m^{-1} as extinction value, the right one results in 6.66 m^{-1} as final value. Close examination of the data reveals that in the right graph values around a depth of 0.4 m are much better represented by the result than in both the middle and left graph. Data for station 6 (the turbid Dollard area) at 2012-dec-16.

C.4. Eilers-Peeters equation

Productivity-light (PI) curves for each sample were fitted using the model by Eilers and Peeters (Eilers and Peeters, 1988):

$$PP = \frac{I}{aI^2 + bI + c} \quad \left(\text{mg C (mg chla)}^{-1}\ \text{h}^{-1}\right) \tag{C2}$$

with I for the actual light intensity (μE m^{-2} s^{-1}).

Parameters a, b and c are computed using a non-linear least squares -routine (NLS) (Bates and Chambers, 1992) from the R-library (R Core Team, 2021).

These parameters a, b and c are nothing more than model parameters. The a-parameter allows for an optimum in the PI-curve, and the c-parameter determines the initial slope of the PI-curve. At I-> 0, the denominator equals c, and thus if follows that.

$$PP = \frac{I}{c} = \alpha^B \quad I\left(\text{mg C (mg chla)}^{-1}\ \text{h}^{-1}\right) \tag{C2a}$$

And thus, the initial slope is 1/c (or: α^B) (mg C (mg chla)$^{-1}$ h^{-1} (μE m^{-2} s^{-1})$^{-1}$), or 278 times (10^6/3600) this value when in mg C (mol photon)$^{-1}$ s^{-1}.

Both parameters a and b determine, together with c, the maximum potential photosynthetic production rate.

$$P_{max} = \frac{1}{2\sqrt{ac} + b} \quad \left(\text{mg C mg}^{-1}\ \text{chla h}^{-1}\right) \tag{C3}$$

C.5. Conversion factors for light and productivity

Partly, light data in this research are in μE m^{-2} s^{-1} (incubation experiments, underwater light climate analysis) while others are in W m^{-2} (such as the solar radiation data available from the Royal Netherlands Meteorological Institute (KNMI, 2021)).

A well-established conversion factor from W m^{-2} to μE m^{-2} s^{-1} is 4.76 (μmol J^{-1}) Langhans and Tibbitts, 1997). The conversion from total available radiation to its photoactive part (PAR) is due to discussion. Golterman (1975) mentioned 0.5, as did Purchase et al. (2015). Miller (1981) mentions a factor ranging from 0.42 for direct sunlight to 0.65 for diffuse radiation. From solar radiation (W m^{-2}) to PAR (in μE m^{-2} s^{-1}) it implies a factor of 1.99 to 3.09 (with as arithmetic average 2.54), and 2.38 if following Golterman (1975) and Purchase et al. (2015). Although García-Rodríguez et al. (2020) argued, based on open air spectral analysis, that this value is an overestimation, and should be 1.93 (μmol J^{-1}), we used a

conversion of 1 W $m^{-2} \approx 2.52$ µE m^{-2} s^{-1} (= µmol J^{-1}), which is according to the previous values.

Productivity units may differ per publication. Generally, mg C (mg chla)$^{-1}$ h^{-1} (µE m^{-2} s^{-1})$^{-1}$ is applied. It contains the dimension time twice; and therefore, this can be eliminated and results then are expressed as mg C (mg chla)$^{-1}$ (E m^{-2})$^{-1}$. The conversion factor that applies is mg C (mg chla)$^{-1}$ (E m^{-2})$^{-1}$ = 278 * mg C (mg chla)$^{-1}$ h^{-1} (µE m^{-2} s^{-1})$^{-1}$.

C.6. Effects of temperature and nutrients

The set-up of the study primarily focussed on the primary production of the Ems-Dollard system, and not finding a relationship between primary productivity and nutrient concentrations or temperature. Nevertheless, we checked whether available nutrient and temperature data could give a better idea of the role of temperature and nutrients.

We tested several possible relationships between α^B and P^B_{max} (steepness and maximum values of the PI-curves, respectively) and temperature (T), nutrient concentrations [N] and combinations of these with algae group dominance. Consistent with literature (Lampert and Sommer, 1993), there was no relationship of α^B with T. P^B_{max} as well as I_{max} (the light intensity at which P^B_{max} was found during the incubation experiments) showed an increase with T, although with a high variability (Fig. 9). Attempts to find some significant relationship of α^B or P^B_{max} with [N] (whether P, Si or N) failed; this can be attributed to the fact that nutrient limitation probably only occurs in a very few cases out of the roughly 230 data points.

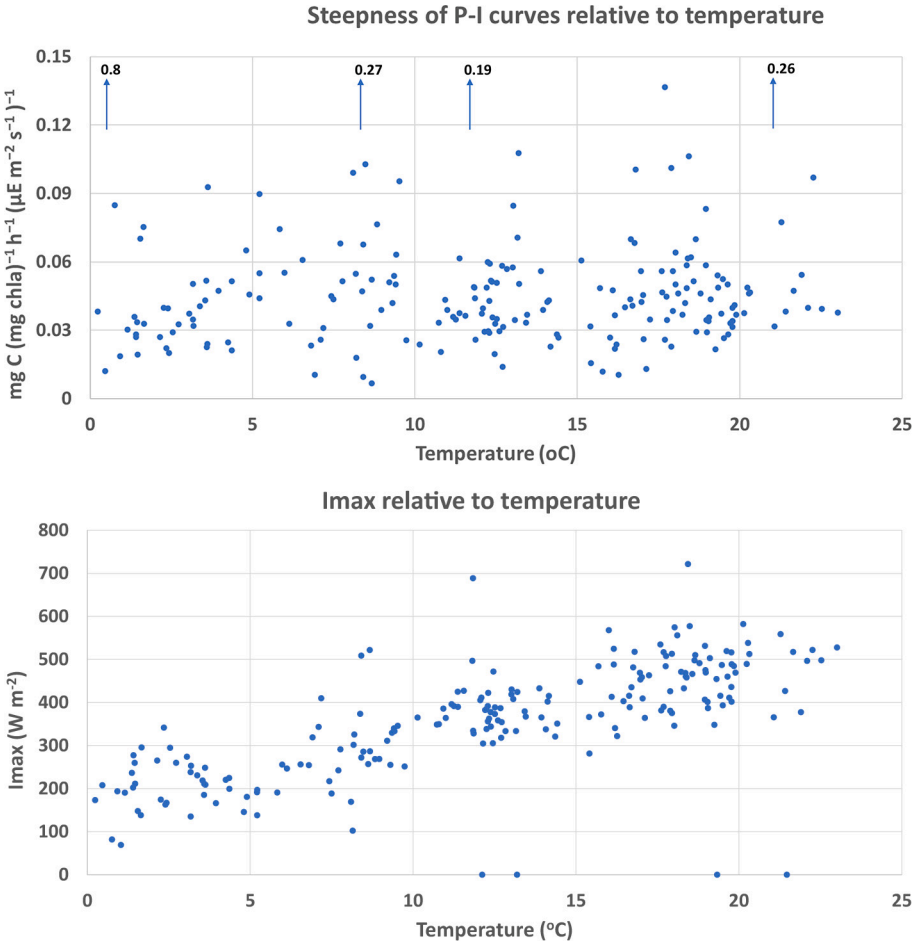

Fig. C2. Eilers-Peeters parameters related to temperature. Upper: α^B, steepness of P-I-curve at low light intensities, indicating no relationship. Four values are considered as outliers, one of these, the large value (0.8 mg C (mg chla)$^{-1}$ h^{-1} (µmol photons m^{-2} s^{-1})$^{-1}$, at 1.1 °C, 2012-02-16, station 1) was considered an experimental error. Lower: I_{max}, the light intensity (W m^{-2}) at which P^B_{max} was found.

Appendix D. Details

D.1. Contour plots

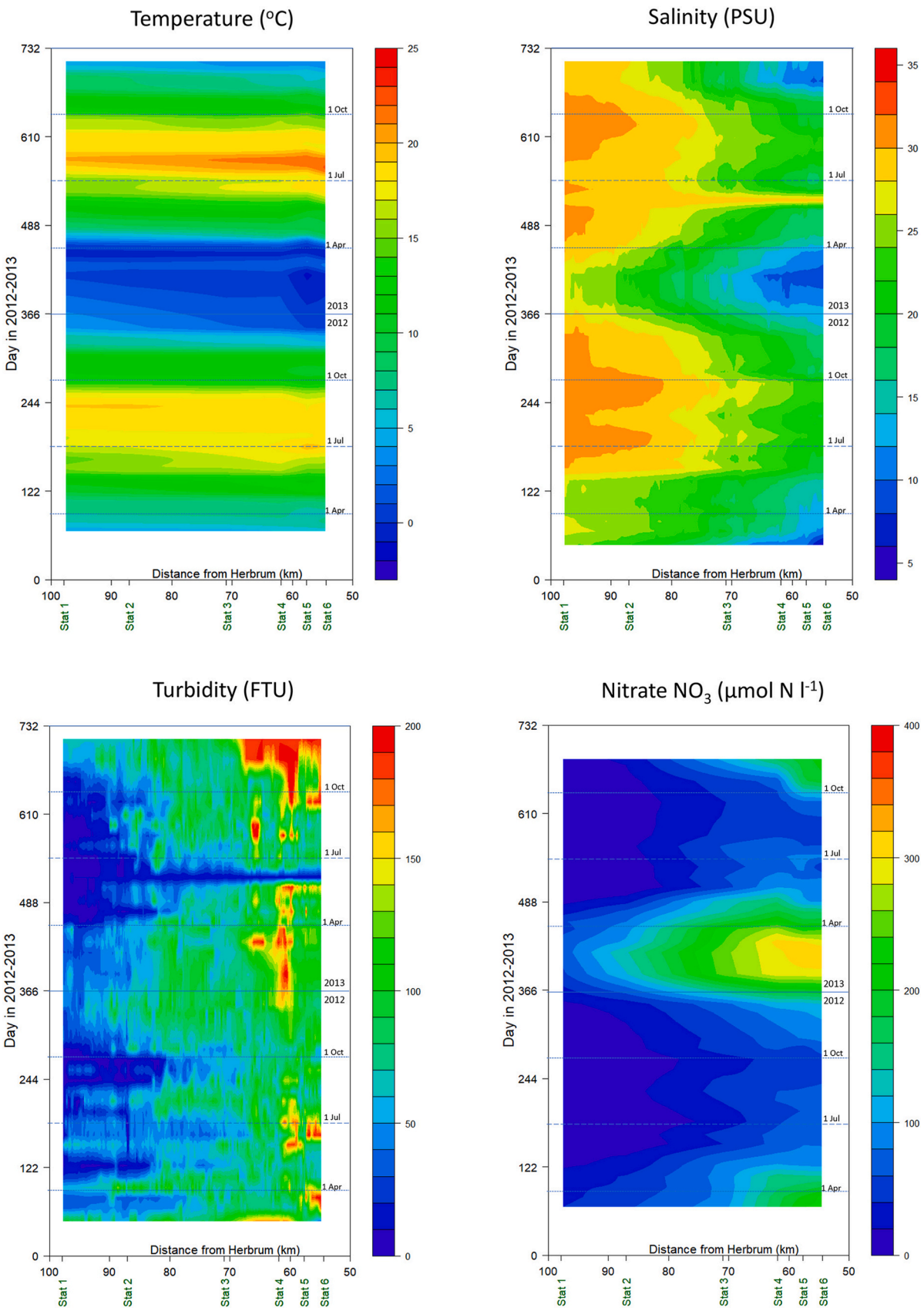

Fig. D1. Contour plots. Upper left: temperature (°C), upper right: salinity (PSU), lower left: turbidity (FTU), lower right: nitrate NO_3-N (µmol N l^{-1}) in the estuary in 2012–2013 (lower to top) at 1 m depth. Stations are mentioned, as is the distance from the Ems-river weir at Herbrum.

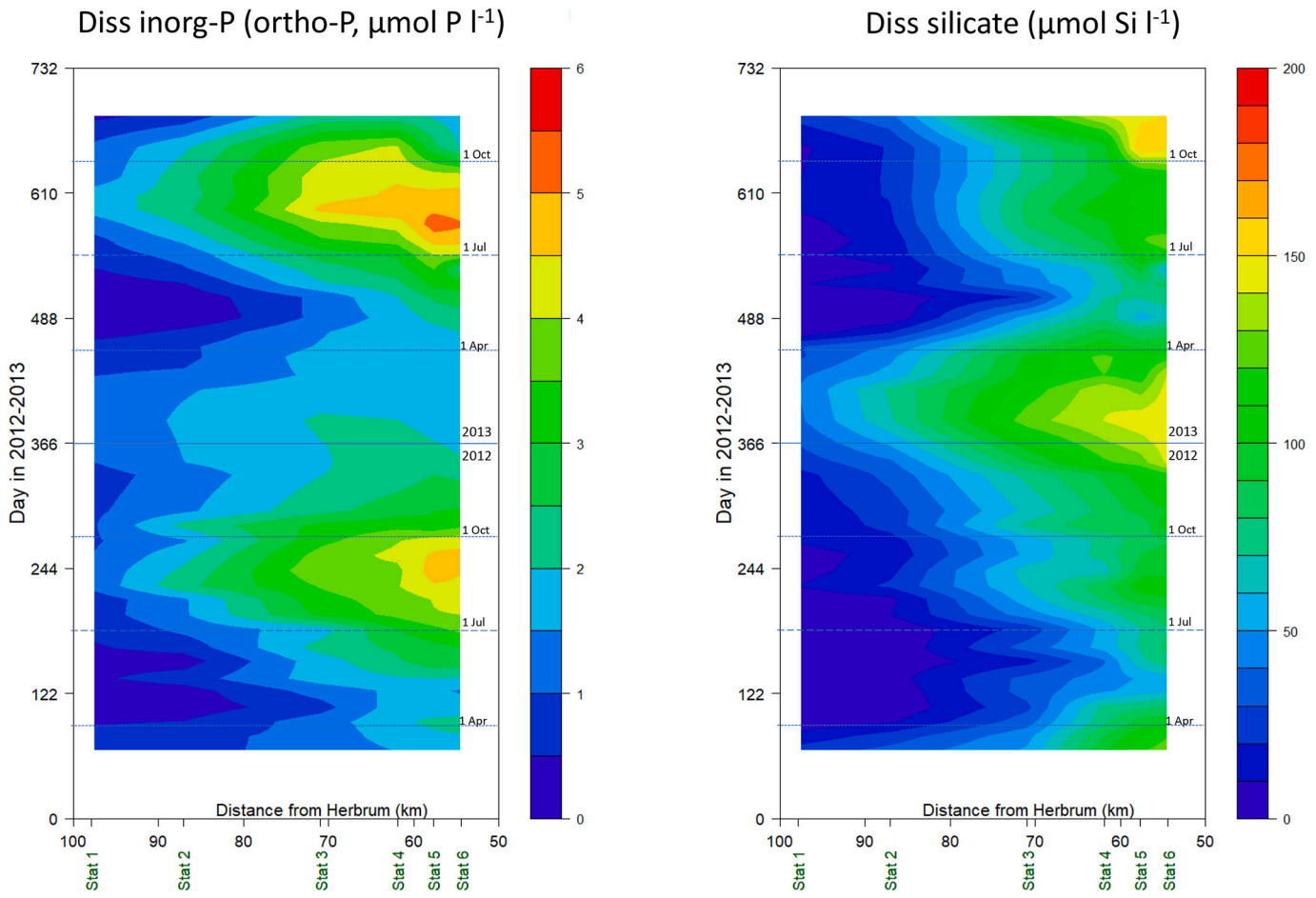

Fig. D2. Contour plots. Left: dissolved inorganic phosphorus (ortho-P, µmol P l^{-1}), right: dissolved silicate (µmol Si l^{-1}) in the estuary in 2012–2013 (lower to top) at 1 m depth. Stations are mentioned, as is the distance from the Ems-river weir at Herbrum.

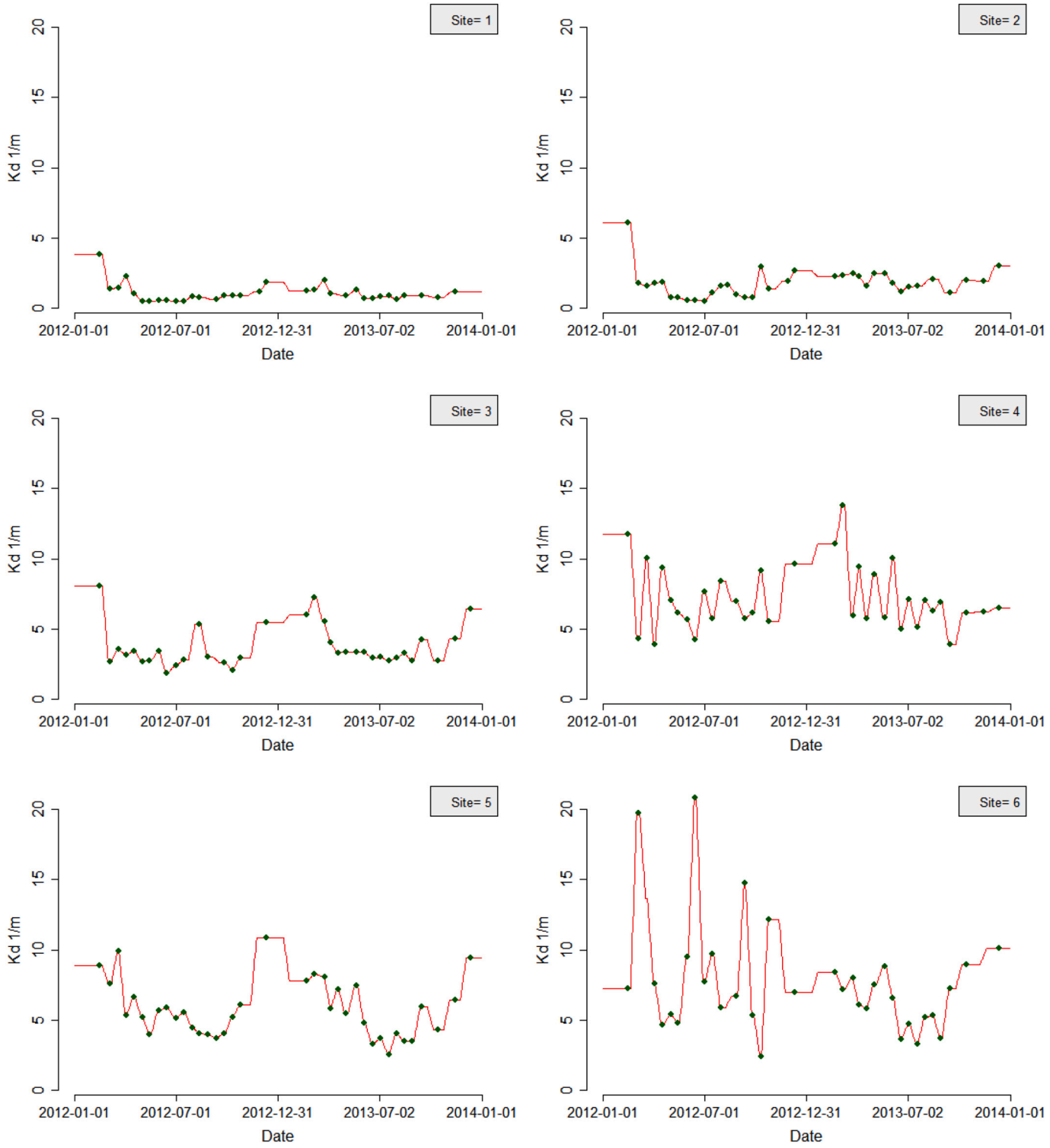

Fig. D3. Light attenuation coefficients K_d (m^{-1}) in 2012–2013 at all six stations (Fig. 1). A moving average interpolation method was applied for data interpolation.

D.2. Light attenuation values for all stations

D.2.1. Production details per station and per compartment

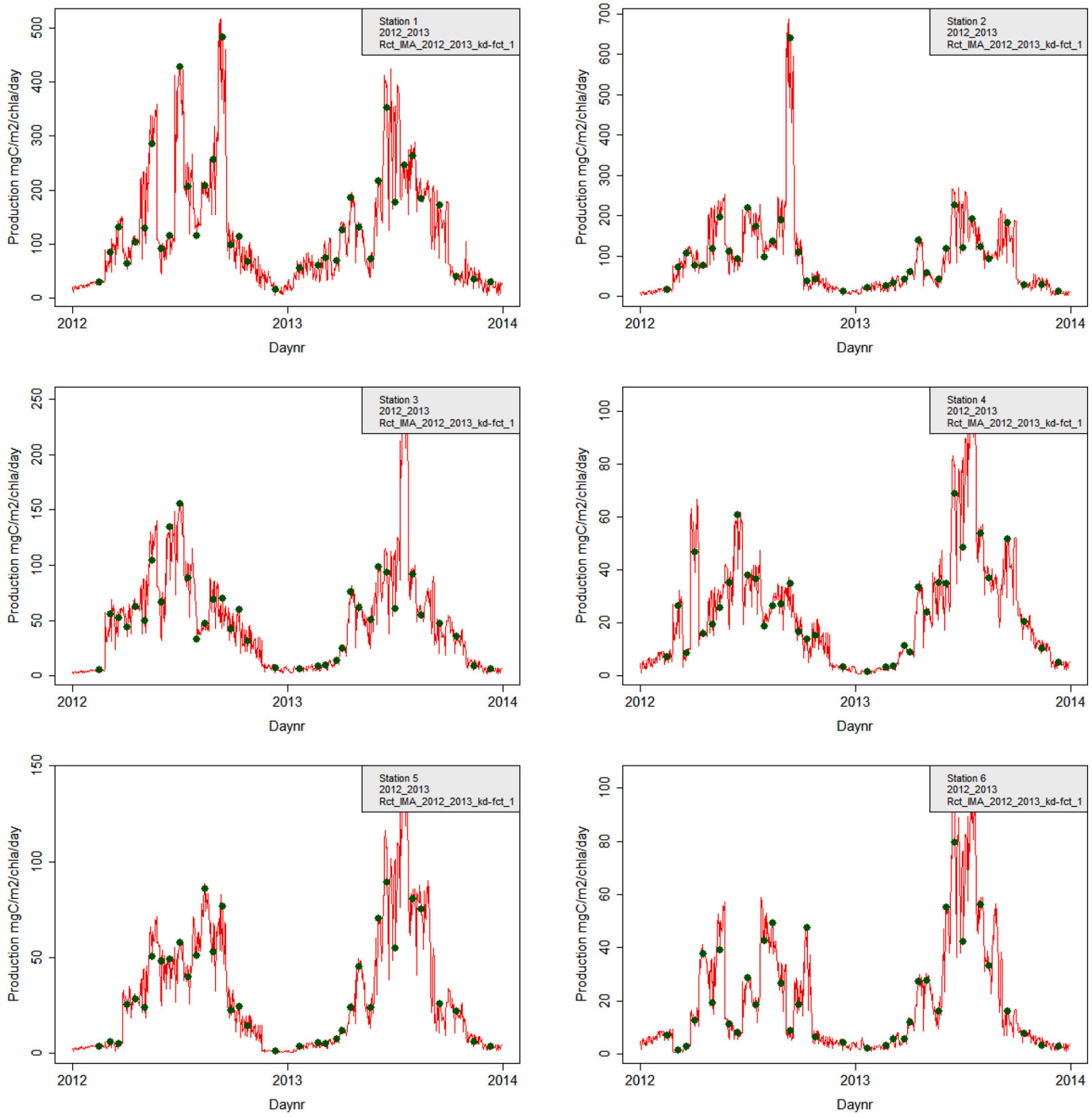

Fig. D4. Productivity results for 2012–2013 (as mg C (mg chla)$^{-1}$ m^{-2} d^{-1}), for each station. Based on ambient temperatures and solar radiation plus the photosynthetic parameters as found during the incubation experiments. Depth and light attenuation conditions are not accounted for.

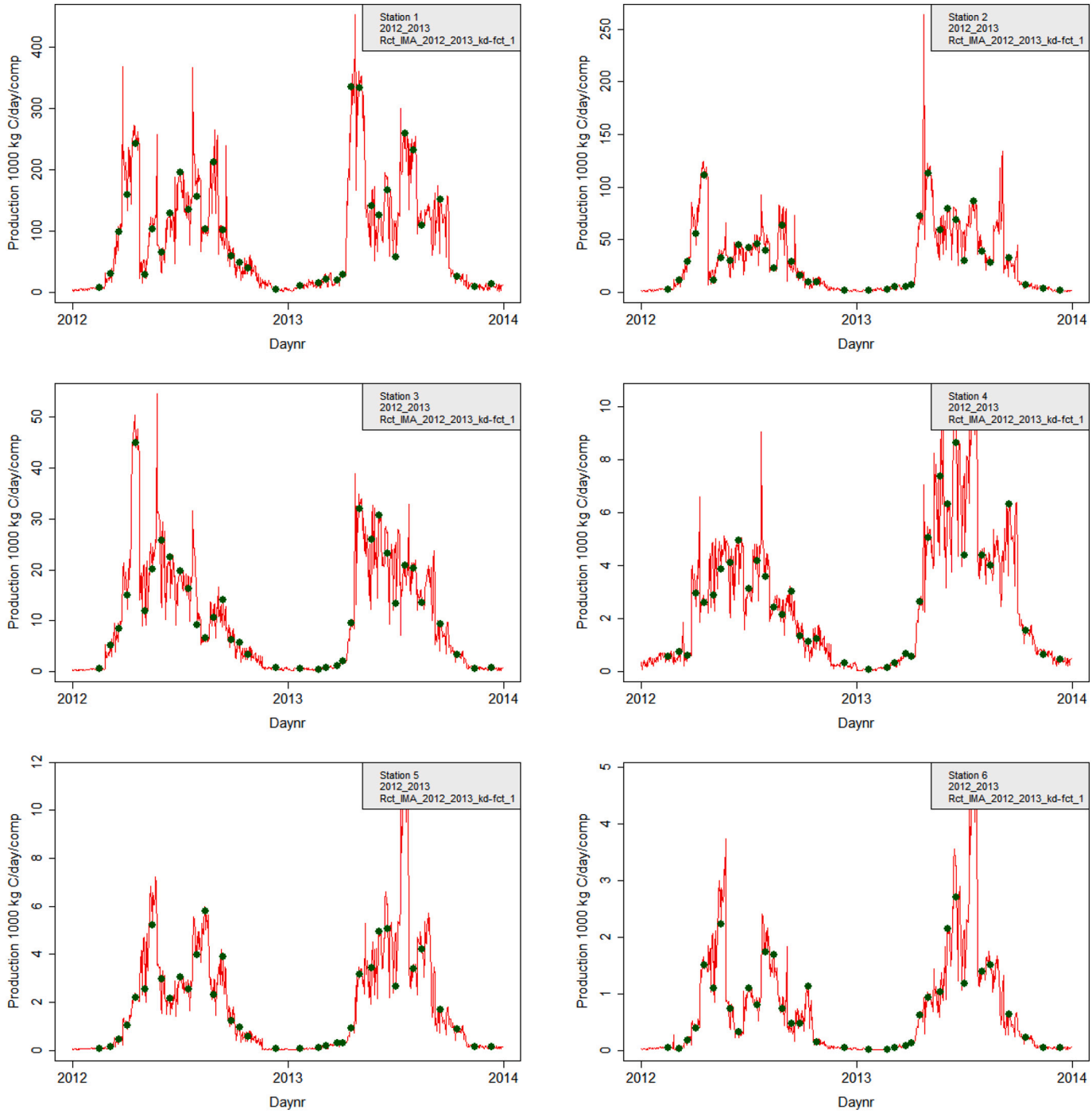

Fig. D5. Compartment integrated productivity results for 2012–2013 (as 1000 kg C comp^{-1} d^{-1}), based on the photosynthetic parameters as found during the incubation experiments plus ambient temperatures, solar radiation, depth and light attenuation conditions.

D.2.2. Production summary for tidal flats and for channels

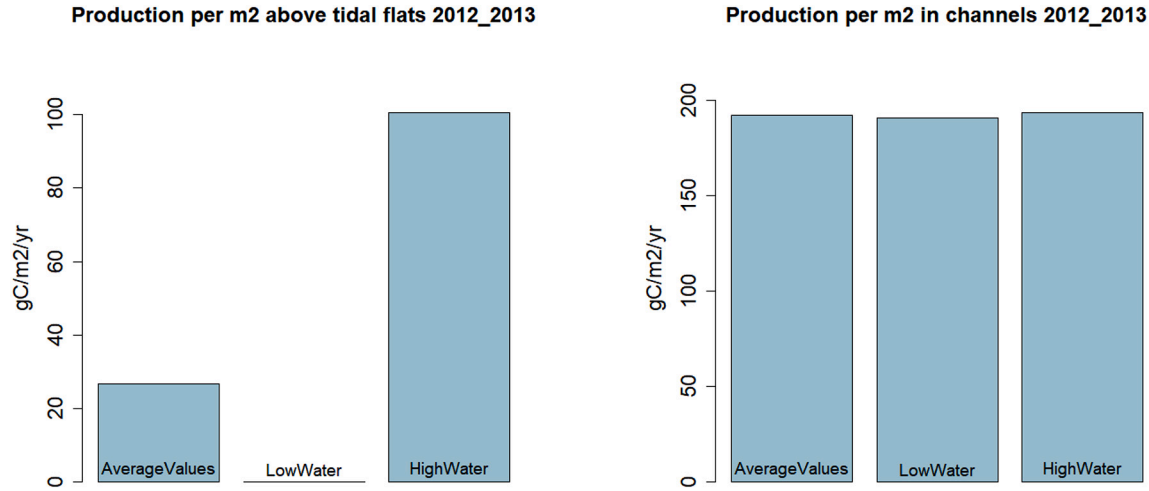

Fig. D6. Production results for 2012–2013 (as g C m^{-2} y^{-1}), based on ambient temperatures, solar radiation and field chlorophyll-a data, plus the photosynthetic parameters as found during the incubation experiments. Results are for tidal flats (left) and channels (right), during high and low water, and as average. Different scales for channels and tidal flats.

References

4h-Jena Engineering, 2021. https://www.4h-jena.de/en/maritime-technologies/flow-systems/pocketferrybox/.

Asmus, R., Jensen, M.H., Murphy, D., Doerffer, R., 1998. Primary production of Microphytobenthos, phytoplankton and the annual yield of macrophytic biomass in the Sylt-Rømø Wadden Sea. In: Gätje, Ch., Reise, K. (Eds.), Ökosystem Wattenmeer. Austausch- Transport- und Stoffumwandlungsprozesse. Chapter 3.3.1. Springer, Berlin.

Baretta, J., Ruardij, P., 1988. Tidal flat estuaries. Springer Verlag, Berlin, p. 353.

Bates, D.M., Chambers, J.M., 1992. *Nonlinear models,* chapter 10 in. In: Chambers, J.M., Hastie, T.J. (Eds.), Statistical Models in S. Wadsworth and Brooks/Cole.

Behrenfeld, M.J., Prasil, O., Babin, M., Bruyant, F., 2004. In search of a physiological basis for covariations in light-limited and light-saturated photosynthesis 1. J. Phycol. 40 (1), 4–25.

Beukema, J.J., Cadée, G.C., Dekker, R., 2002. Zoobenthic biomass limited by phytoplankton abundance: evidence from parallel changes in two long-term data series in the Wadden Sea. J. Sea Res. 48, 111–125.

Bode, A., Varela, M., 1998. Primary production and phytoplankton in three Galician rias Altas (NW Spain): seasonal and spatial variability. Sci. Mar. 62 (4), 319–330.

Bot, P.V.M., Colijn, F., 1996. A method for estimating primary production from chlorophyll concentrations with results showing trends in the Irish Sea and the Dutch coastal zone. ICES J. Mar. Res. 53, 945–950.

Bouman, H., Platt, T., Sathyendranath, S., Stuart, V., 2005. Dependence of light-saturated photosynthesis on temperature and community structure. Deep Sea Res. Part I: Oceanograph. Res. Papers 52 (7), 1284–1299.

Bouman, H.A., Platt, T., Doblin, M., Figueiras, F.G., Gudmundsson, K., Gudfinnsson, H. G., Huang, B., Hickman, A., Hiscock, M., Jackson, T., Lutz, V.A., Mélin, F., Rey, F., Pepin, P., Segura, V., Tilstone, G.H., Van Dongen-Vogels, V., Sathyendranath, S., 2018. Photosynthesis–irradiance parameters of marine phytoplankton: synthesis of a global data set. Earth Syst. Sci. Data. 10, 251–266.

Brinkman, A.G., 2008. Nutriënt- en Chlorofylgehaltes in Het Westelijke en Oostelijke Deel van de Nederlandse Waddenzee; Waarden en Trends Tussen 1980 en 2005 en Mogelijke Oorzaken Daarvan. Wageningen IMARES Texel, rapport C112/08, p. 365 (rapp+app). https://www.wur.nl/nl/Publicatie-details.htm?publicationId=publication-way-333739313135.

Brinkman, A.G., Riegman, R., Jacobs, P., Kuhn, S., Meijboom, A., 2014. Ems-Dollard Primary Production Research Full Data Report. IMARES Wagening UR Report C160/14. https://www.wur.nl/nl/Publicatie-details.htm?publicationId=publicatio n-way-343839373039.

Cadée, G.C., Hegeman, J., 1974. Primary production of phytoplankton in the Dutch Wadden Sea. Neth. J. Sea Res. 8 (3), 240–259.

Cadée, G.C., Hegeman, J., 1993. Persisting high levels of primary production at declining phosphate concentrations in the Dutch coastal area (Marsdiep). Neth. J. Sea Res. 31 (2), 147–152.

Claquin, P., Longphuirt, S.N., Fouillaron, P., Huonnic, P., Ragueneau, O., Klein, C., Leynaert, A., 2010. Effects of simulated benthic fluxes on phytoplankton dynamic and photosynthetic parameters in a mesocosm experiment (bay of Brest, France). Estuar. Coast. Shelf Sci. 86 (1), 93–101.

Cloern, J.E., 1987. Turbidity as a control on phytoplankton biomass and productivity in estuaries. Cont. Shelf Res. 7 (11−12), 1367–1381.

Colijn, F., 1982. Light absorption in the waters of the Ems-Dollard estuary and its consequences for the growth of phytoplankton and microphytobenthos. Neth. J. Sea Res. 15 (2), 196–216.

Colijn, F., 1983. Primary Production in the Ems-Dollard estuary. Ph. D. Thesis, Groningen, The Netherlands, p. 123.

Compton, T.J., Holthuijsen, S., Koolhaas, A., Dekinga, A., Ten Horn, J., Smith, J., Galama, Y., Brugge, M., Van der Wal, D., Van der Meer, J., Van der Veer, H.W., 2013. Distinctly variable mudscapes: distribution gradients of intertidal macrofauna across the Dutch Wadden Sea. J. Sea Res. 82, 103–116.

Compton, T.J., Holthuijsen, S., Mulder, M., Van Arkel, M., Kleine Schaars, L., Koolhaas, A., Dekinga, A., Ten Horn, J., Luttikhuizen, P.C., Van der Meer, J., Piersma, Th., Van der Veer, H.W., 2017. Shifting baselines in the Ems-Dollard estuary: a comparison across three decades reveals changing benthic communities. J. Sea Res. 127, 117–132. https://doi.org/10.1016/j.seares.2017.06.014.

Côté, B., Platt, T., 1983. Day-to-day variations in the spring-summer photosynthetic parameters of coastal marine phytoplankton. Limnol. Oceanogr. 28, 320–344.

De Jonge, V.N., Brauer, V.S., 2006. The Ems Estuary: Changes in Functioning and Structure of a System Under Pressure. Report RUG 7032007, p. 99.

De Jonge, V.N., Schückel, U., 2019. Exploring effects of dredging and organic waste on the functioning and the quantitative biomass structure of the Ems estuary food web by applying input model balancing in ecological network analysis. Ocean Coast. Manag. 174, 38–55.

De Jonge, V.N., Schuttelaars, H.M., Van Beusekom, J.E.E., Talke, S.A., De Swart, H.E., 2014. The influence of channel deepening on estuarine turbidity levels and dynamics, as exemplified by the Ems estuary. Estuar. Coast. Shelf Sci. 139, 46–59.

EasyGSh-DB Projekt, 2020. https://mdi-de.baw.de/easygsh/index.html#home.

ED2050, 2021. Programma Plan Eems-Dollard 2050, 2021–2026. https://eemsdollard2050.nl/english/why-this-program/.

Eggink, H., 1965. Het Estuarium als Ontvangend Water van Grote Hoeveelheden Afvalstoffen. Rijksinstituut Voor Zuivering van Afvalwater, Med.Nr 2.

Eilers, P.H.C., Peeters, J.C.H., 1988. A model for the relationship between light intensity and the rate of photosynthesis in phytoplankton. Ecol. Model. 42, 199–215.

Essink, K., 1978. The Effects of Pollution by Organic Waste on Macrofauna in the Eastern Dutch Wadden Sea. PhD-Thesis. RU Groningen, p. 135.

Essink, K., 2003. Response of an estuarine ecosystem to reduced organic waste discharge. Aquatic Ecol. 37 (1), 65–76.

Essink, K., Esselink, P., 1998. Het Eems-Dollard Estuarium: Interacties Tussen Menselijke Beïnvloeding en Natuurlijke Dynamiek. Rijkswaterstaat, Rapport RIKZ-98, p. 020.

Falkowski, P.G., 1981. Light-shade adaptation and assimilation numbers. J. Plankton Res. 3, 203–216.

Falkowski, P.G., Raven, J.A., 1997. Aquatic Photosynthesis. Blackwell, Oxford.

Galatius, A., Brasseur, S., Carius, F., Jeß, A., Meise, K., Meyer, J., Schop, J., Siebert, U., Stejskal, O., Teilmann, J., Thøstesen, C.B., 2022. Survey Results of Harbour Seals in the Wadden Sea in 2022. Common Wadden Sea Secretariat, Wilhelmshaven, Germany.

García-Rodríguez, A., García-Rodríguez, S., Díez-Mediavilla, M., Alonso-Tristán, C., 2020. Photosynthetic active radiation, solar irradiance and the CIE standard sky classification. Appl. Sci. 10 (22), 8007. https://doi.org/10.3390/app10228007.

Golterman, H.L., 1975. Physiological Limnology. Elsevier Scient. Publ, Comp, p. 489.

Groen, P., 1967. On the residual transport of suspended matter by an alternating tidal current. Neth. J. Sea Res. 3, 564–574.

Hach, 2012a. http://www.hach.com/hq40d-portable-ph-conductivity-optical-dissolved-oxygen-do-orp-and-ise-multi-parameter-meter/.Conductivity and salinity product-parameter-reagent?id=7640501639.

Hach, 2012b. http://www.hach.com/intellical-ldo101-rugged-luminescent-optical-dissolved-oxygen-ldo-probe-5-meter-cable/product-details?id=7640489865.

Heath, M.F., Evans, M.I. (Eds.), 2000. Important Bird Areas in Europe; Priority Sites for Conservation I: Northern Europe. Birdlife International (BirdLife Conservation Series No 8). Cambridge.
Herbert, A., 1999. Nitrogen cycling in coastal marine ecosystems. FEMS Microbiol. Rev. 23, 563–590.
Holm-Hansen, O., Lorenzen, C.J., Holms, R.W., Strickland, J.D.H., 1965. Fluorometric determination of chlorophyll. J. Cons. Perms. Int. Explor. Mer. 30, 3–15.
Jacobs, P., Kromkamp, J.C., Van Leeuwen, S.M., Philippart, C.J.M., 2020. Planktonic primary production in the western Dutch Wadden Sea. Mar. Ecol. Prog. Ser. 639, 53–71.
Jacobs, P., Pitarch, J., Kromkamp, J.C., Philippart, C.J., 2021. Assessing biomass and primary production of microphytobenthos in depositional coastal systems using spectral information. PLoS One 16 (7), e0246012.
Kennish, M.J., 2002. Environmental threats and environmental future of estuaries. Environ. Conserv. 29, 78–107.
Kirk, J.T.O., 1994. Light and Photosynthesis in Aquatic Ecosystems, 2nd ed. Cambridge Univ. Press, p. 509.
KNMI, 2021. Royal Netherlands Meteorological Institute. Hourly meteorological data.
Kromkamp, J.C., Van Engeland, T., 2010. Changes in phytoplankton biomass in the Western Scheldt estuary during the period 1978-2006. Estuar. Coasts 33, 270–285. https://doi.org/10.1007/s12237-009-9215-3.
Lampert, W., Sommer, U., 1993. Limnoökologie. Georg Thieme Verlag Stuttgart, p. 439.
Plant Growth Chamber Handbook. In: Langhans, R.W., Tibbitts, T.W. (Eds.), 1997. North Central Regional Research Publication No. 340; Iowa Agriculture and Home Economics Experiment Station Special Report No. 99. https://www.controllede nvironments.org/wp-content/uploads/sites/6/2017/06/Ch01.pdf.
Licor, 2022. https://www.licor.com/env/products/light/.
Loebl, M., Dolch, T., Van Beusekom, J.E., 2007. Annual dynamics of pelagic primary production and respiration in a shallow coastal basin. J. Sea Res. 58 (4), 269–282.
Lohrenz, S.E., Fahnenstiel, G.L., Redalje, D.G., 1994. Spatial and temporal variations of photosynthetic parameters in relation to environmental conditions in coastal waters of the northern Gulf of Mexico. Estuaries. 17, 779–795.
Lohse, L., Malschaert, J.F.P., Slomp, C.P., Helder, W., Van Raaphorst, W., 1993. Nitrogen cycling in North Sea sediments: interaction of denitrification and nitrification in offshore and coastal areas. Mar. Ecol. Prog. Ser. 101, 283–296.
Mangoni, O., Carrada, G.C., Modigh, M., Catalano, G., Saggiomo, V., 2009. Photoacclimation in Antarctic bottom ice algae: an experimental approach. Polar Biol. 32 (3), 325–335.
Miller, D.H. (Ed.), 1981. Energy at the Surface of the Earth: An Introduction to the Energetics of Ecosystems, Ch 5: Total Incoming Solar Radiation. International Geophysics, 27. Academic Press, pp. 71–95.
Napoléon, C., Raimbault, V., Fiant, L., Riou, P., Lefebvre, S., Lampert, L., Claquin, P., 2012. Spatiotemporal dynamics of physicochemical and photosynthetic parameters in the Central English Channel. J. Sea Res. 69, 43–52.
OSM. https://www.openstreetmap.org/.
Platt, T., Jassby, A.D., 1976. The relationship between photosynthesis and light for natural assemblages of coastal marine phytoplankton 1. J. Phycol. 12, 421–430.
Post, A.F., de Wit, R., Mur, L.R., 1985. Interactions between temperature and light intensity on growth and photosynthesis of the cyanobacterium *Oscillatoria agardhii*. J. Plankton Res. 7 (4), 487–495.
Postma, H., 1961. Transport and accumulation of suspended matter in the Dutch Wadden Sea. Neth. J. Sea Res. 1, 148–190.
Pritchard, D.W., 1967. What is an estuary: physical standpoint. In: Lauff, G.H. (Ed.), Estuaries, 83. American Association for the Advancement of Science, Publication, Washington, DC, USA, pp. 3–5.
Artificial Photosynthesis, for the Conversion of Sunlight to Fuel. Biophysical Organic Chemistry/Solid State NMR. In: Purchase, R., De Vriend, H., De Groot, H., Harmsen, P., Bos, H. (Eds.), 2015. Leiden Institute of Chemistry and Wageningen UR Food and Biobased Research.
R Core Team, 2021. R: A Language and Environment for Statistical Computing. R Foundation for Statistical Computing, Vienna, Austria. ISBN 3–900051–07-0, URL. http://www.R-project.org/.
Riegman, R., Colijn, F., 1991. Evaluation of measurements and calculation of primary production in the Dogger Bank area (North Sea) in summer 1988. Mar. Ecol. Prog. Ser. 69, 125–132.
Riegman, R., Colijn, F., Malschaert, J.F.P., Kloosterhuis, H.T., Cadée, G.C., 1990. Assessment of growth rate limiting nutrients in the North Sea by the use of nutrient-uptake kinetics. Neth. J. Sea Res. 26 (1), 53–60.
RIKZ, 1998. Sedimentatlas Waddenzee. Ministerie van Verkeer en Waterstaat/ Rijksinstituut voor Kust en Zee.
RWS, 2017. Water Monitoring Data Rijkswaterstaat. https://waterinfo.rws.nl/.
Sakshaug, E., Bricaud, A., Dandonneau, Y., Falkowski, P.G., Kiefer, D.A., Legendre, L., Morel, A., Parslow, J., Takahashi, M., 1997. Parameters of photosynthesis: definitions, theory and interpretation of results. J. Plankton Res. 19 (11), 1637–1670.
Sathyendranath, S., Longhurst, A., Caverhill, C.M., Platt, T., 1995. Regionally and seasonally differentiated primary production in the North Atlantic. Deep-Sea Res. 42, 1773–1802.
Schuttelaars, H.M., De Jonge, V.N., Chernetsky, A., 2013. Improving the predictive power when modelling physical effects of human interventions in estuarine systems. Ocean Coast. Manag. 79, 70–82.
Strickland, J.D.H., Parsons, T.R., 1972. A practical handbook of seawater analysis. Bull. Fish. Res. Board Can. Second Edition 167, 267–278.
Talke, S.A., De Swart, H.E., 2006. Hydrodynamics and Morphology in the Ems/Dollard Estuary: Review of Models, Measurements, Scientific Literature, and the Effects of Changing Conditions, 87. Civil and Environmental Engineering Faculty Publications and Presentations. https://pdxscholar.library.pdx.edu/cengin_fac/87.
Talke, S.A., De Swart, H.E., 2011. Circulation, sediment concentration and oxygen depletion in the tidal Ems River. In: Heip, C., et al. (Eds.), Aspects of coastal research in contribution to LOICZ in the Netherlands and Flanders (2002–2010), 38. LOICZ Research and Studies, pp. 42–48.
Tillmann, U., Hesse, K.J., Colijn, F., 2000. Planktonic primary production in the German Wadden Sea. J. Plankton Res. 22 (7), 1253–1276.
Van Arkel, M.A., 1977. Some results of a survey of the macrobenthic fauna of the Ems-Dollard estuary (Eastern Dutch Wadden Sea). Hydrobiol. Bull. 11, 15–16.
Van Asch, M., Van den Ende, D., Brummelhuis, E.B.M., Van Zweeden, C., Troost, K., 2015. Het Kokkelbestand in de Nederlandse Kustwateren in 2015. IMARES Wageningen UR Report C111/15, Wageningen/ Yerseke.
Van den Ende, D., Troost, K., Van Stralen, M., Van Zweden, C., Van Asch, M., 2012. Het Mosselbestand en Het Areaal Aan Mosselbanken op de Droogvallende Platen van de Waddenzee in Het Voorjaar Van 2012. IMARES Wageningen-UR Report C149/12, Wageningen/ Yerseke, p. 26.
Van Maren, D.S., van Kessel, T., Cronin, K., Sittoni, L., 2015. The impact of channel deepening and dredging on estuarine sediment concentration. Cont. Shelf Res. 95, 1–14.
Van Maren, D.S., Oost, A.P., Wang, Z.B., Vos, P.C., 2016. The effect of land reclamations and sediment extraction on the suspended sediment concentration in the Ems estuary. Mar. Geol. 376, 147–157. https://doi.org/10.1016/j.margeo.2016.03.007.
Van Raaphorst, W., De Jonge, V.N., 2004. Reconstruction of the total N and P inputs from the IJsselmeer into the western Wadden Sea between 1935-1998. J. Sea Res. 51, 109–131.
Waltz, 2022. https://www.walz.com/products/light/us-sqs_l/introduction.html.
Wang, Z.B., Hoekstra, P., Burchard, H., Ridderinkhof, H., De Swart, H.E., Stive, M.J.F., 2012. Morphodynamics of the Wadden Sea and its barrier island system. Ocean Coast. Manag. 68, 39–57.
Wang, Z., Elias, E., van der Spek, A., Lodder, Q., 2018. Sediment budget and morphological development of the Dutch Wadden Sea: impact of accelerated sea-level rise and subsidence until 2100. Neth. J. Geosci. Geol. Mijnb. 97, 183–214. https://doi.org/10.1017/njg.2018.8.
Wetlabs, 2012. http://www.wetlabs.com.
Zheng, Z.-Z., Wan, X., Xu, M.N., Hsiao, S.S.-Y., Zhang, Y., Zheng, L.-W., Wu, Y., Zou, W., Kao, S.-J., 2017. Effects of temperature and particles on nitrification in a eutrophic coastal bay in southern China. J. Geophys. Res. Biogeosci. 122, 2325–2337. https://doi.org/10.1002/2017JG003871.